Reference Values for Pulse Wave Doppler and Tissue Doppler Imaging in Pediatric Echocardiography

Frederic Dallaire, MD, PhD; Cameron Slorach, RDSC; Wei Hui, MD; Taisto Sarkola, MD, PhD; Mark K. Friedberg, MD; Timothy J. Bradley, MBChB; Edgar Jaeggi, MD; Andreea Dragulescu, MD, PhD; Ronnie L.H. Har, MSc; David Z.I. Cherney, MD, PhD; Luc Mertens, MD, PhD

Background—In pediatric echocardiography, pulse wave Doppler, and tissue Doppler imaging velocities are widely used to assess cardiac function. Current reference values and *Z* scores, allowing adjustment for growth are limited by inconsistent methodologies and small sample size. Using a standardized approach for parametric modeling and *Z* score quality assessment, we propose new pediatric reference values and *Z* score equations for most left ventricular pulse wave Doppler and tissue Doppler imaging measurements.

Methods and Results—Two hundred thirty-three healthy pediatric subjects 1 to 18 years of age were prospectively recruited. Thirteen pulse wave Doppler and 14 tissue Doppler imaging measurements were recorded. Normalization for growth was done via a complete and standardized approach for parametric nonlinear regression modeling. Several analyses were performed to ensure adequate *Z* score distribution and to detect potential residual associations with growth or residual heteroscedasticity. Most measurements adopted a nonlinear relationship with growth and displayed significant heteroscedasticity. Compared with age, height, and weight, normalization for body surface area was most efficient in removing the effect of growth. Generally, polynomial and allometric models yielded adequate goodness-of-fit. Residual values for several measurements had significant departure from the normal distribution, which could be corrected using logarithmic or reciprocal transformation. Overall, weighted parametric nonlinear models allowed us to compute *Z* score equations with adequate normal distribution and without residual association with growth.

Conclusions—We present *Z* scores for normalized pulse wave Doppler and tissue Doppler imaging in pediatric echocardiography. Further studies are needed to define the threshold beyond which health becomes a disease by integrating other important factors such as ventricular morphology, loading conditions, and heart rate. **(*Circ Cardiovasc Imaging*. 2015;8:e002167. DOI: 10.1161/CIRCIMAGING.114.002167.)**

Key Words: echocardiography ■ heart failure, diastolic ■ nomograms ■ reference values

Downloaded from http://circimaging.ahajournals.org/ by guest on December 13, 2017

In echocardiography, blood and tissue velocities measured by Doppler are widely used tools for the evaluation of cardiac systolic and diastolic function. In healthy children, many of these parameters vary with growth, often in a nonlinear fashion.[1,2] As recently reviewed by Cantinotti and Lopez,[3] reference values for pulse wave Doppler (PWD) and tissue Doppler imaging (TDI) velocities are often limited by inconsistent methodologies and small sample size. Furthermore, while *Z* scores are becoming the method of choice to normalize echocardiographic measurement in children,[4] standardized methodologies to perform normalization in pediatric echocardiography, especially in the presence of heteroscedasticity and nonlinear relationships, are lacking.[5]

See Clinical Perspective

In this study, we aimed to determine echocardiographic reference values and parametric *Z* scores equations for PWD velocities and TDI velocities in a healthy pediatric population using a complete and standardized approach for regression modeling, detection of residual biases, and assessment of adequate *Z* score distribution.

Methods

Population and Recruitment

Subjects from age 1 to 18 years, without heart disease, were prospectively recruited for this study from local schools, as volunteers and

Received May 23, 2014; accepted December 19, 2014.

From the Division of Pediatric Cardiology, Faculty of Medicine, University of Sherbrooke, Sherbrooke, Quebec, Canada (F.D.); Centre de Recherche du Centre Hospitalier Universitaire de Sherbrooke, Sherbrooke, Quebec, Canada (F.D.); The Labatt Family Heart Centre, Department of Paediatrics, The Hospital for Sick Children, University of Toronto, Toronto, Ontario, Canada (C.S., W.H., T.S., M.K.F., T.J.B., E.J., A.D., L.M.); and Division of Nephrology, Department of Medicine, Toronto General Hospital, University of Toronto, Ontario, Canada (R.L.H.H., D.Z.I.C.).

The Data Supplement is available at http://circimaging.ahajournals.org/lookup/suppl/doi:10.1161/CIRCIMAGING.114.002167/-/DC1.

Correspondence to Frederic Dallaire, MD, PhD, Division of Pediatric Cardiology, Department of Pediatrics, Faculty of Medicine, University of Sherbrooke, 3001, 12e Avenue Nord, Sherbrooke, Quebec, Canada J1H 5N4. E-mail frederic.a.dallaire@usherbrooke.ca

© 2015 American Heart Association, Inc.

also from the Hospital for Sick Children (Toronto, Canada) echocardiography laboratory for children with likely normal cardiac anatomy. Recruitment took place between January 2009 and November 2012. A full anatomic and functional echocardiogram was performed to rule out any abnormalities. Any children with abnormal echocardiographic findings, including minor defects, such as patent foramen ovale and patent ductus arteriosus were automatically excluded from the study. Age, sex, height, and weight were recorded for every patient at the time of the echocardiographic study. Body surface area (BSA) was estimated using the equation proposed by Haycock et al.[6] The Haycock equation was selected because of its closer correlation with echocardiographic measurements in children compared with other published estimations of BSA.[7] Body mass index (BMI) was calculated as weight (kg) ÷ height (m^2) and was normalized for age and sex using the reference standard proposed by the World Health Organization.[8,9] The Institutional Research Ethics Board approved the study and written informed consent was obtained from each participant.

Echocardiographic Examination

We used General Electric's Vivid 7 and E9 (GE, General Electric Corp, Wauwatosa, WI) ultrasound systems for all image acquisitions. The appropriate sectorial transducer was used, ranging from frequencies of 4 to 12 MHz depending on subject age and size. The participants were examined at rest while in the left lateral position during sinus rhythm. All echocardiographic images were acquired using a strictly standardized echocardiographic functional protocol. Echocardiographic acquisitions were performed by 2 experienced research sonographers (C.S., W.H.).

Pulse Wave Doppler

PWD images from 3 cardiac cycles were acquired from an apical 4 chamber view and a sweep speed of 100 cm/s unless stated otherwise. Care was taken to ensure that the ultrasound beam was as parallel as possible to the recorded flow. Appropriate scale and filters were adjusted to optimize the PWD signal and spectral Doppler tracings flow. Peak velocities for E and A waves were measured with a 2 mm sample volume placed at the tips of the mitral valve leaflets. Mitral valve deceleration time was measured as the time from the peak E wave velocity to the cessation of early diastolic flow. Mitral valve closure to mitral valve opening time was measured as the time from the cessation of the mitral A wave flow to the onset of the mitral E wave flow. Aortic left ventricular ejection time was measured in the 5-chamber view with the sample volume immediately below the aortic valve annulus. Aortic left ventricular ejection time was measured as the time from the onset of aortic forward flow to the cessation of aortic forward flow. Left ventricular myocardial performance index was calculated as the ratio of (mitral valve closure to mitral valve opening time−aortic left ventricular ejection time) over aortic left ventricular ejection time. The right upper pulmonary vein was imaged whenever possible to assess pulmonary venous Doppler. A 2 mm sample volume was placed ≈5 mm within the pulmonary vein. Isovolumic relaxation time was measured in the 5-chamber view. A PWD tracing was acquired with the cursor angled to record both the mitral inflow and left ventricular outflow tract. Isovolumic relaxation time was measured as the time from the cessation of the aortic forward flow to the onset of mitral diastolic flow.

Pulse TDI

Pulse TDI images from 3 cardiac cycles were obtained from the apical 4-chamber view at a sweep speed of 100 mm/s. A 5-mm sample volume was used in all subjects placed just below the mitral valve annulus (lateral wall and septum). Gain settings were optimized as needed to avoid aliasing, eliminate background noise and to allow optimal TDI velocity traces. The ultrasound beam was aligned as perpendicular as possible to the interrogated myocardial wall. The sector width was reduced if necessary to obtain high frame rate images of >150 frames per second.

Color TDI

Color coded TDI images from 3 cardiac cycles were obtained from the apical 4-chamber view. The sector width was reduced if necessary to obtain high frame rate images of >150 frames per second. Unaltered uncompressed images were transferred for off-line analysis. Color TDI velocities were measured offline using a GE EchoPAC workstation (General Electric Corp) version 7, from 3 consecutive cardiac cycles by a single sonographer (C.S.). Color TDI velocities were sampled in the same position as the PWD TDI. A 5 mm sample volume was used.

Modelization and *Z* scores

Z scores were computed using a standardized approach for each echocardiographic measurement. We first evaluated the relationship of the dependent variable (measurements) with 4 independent growth variables: height, weight, BSA, and age. In our preliminary analysis, compared with age, height, and weight, we found that normalization for BSA most often yielded *Z* scores with less residual association with other growth parameters. BSA was therefore used as the initial independent normalizing variable. Other growth variables or multivariable models were tested when significant residual association with growth was detected (see below).

Regression models were empirically tested to optimize the goodness-of-fit between the dependent and the independent variables. Linear ($y=ax+b$), allometric ($y=ax^b$), second-order polynomial ($y=ax^2+bx+c$), and third-order polynomial ($y=ax^3+bx^2+cx+d$) models were initially tested. When the fit was deemed inadequate, other models were also assessed: a gamma function model [$y=ax^b\times e^{-cx}$], a polynomial model with the square root of the independent variable ($y=ax+b\sqrt{x}+c$), and multivariable models. Model equations are listed in Table 1. When polynomial models were considered, we were careful to avoid over fitting by consulting scatter plots of previously published articles on healthy patients (see Discussion for references). Such models were considered only if previously published data showed a similar polynomial pattern with growth for a given echocardiographic measurement.

Selection of the most adequate model was based on several factors. We visually appreciated the goodness-of-fit by reviewing graphically the residual values over the independent variable. We then reviewed various fit diagnostic aids, including plots of residuals over predicted values, plots of residuals over quantiles, distribution of residuals and proportion less plots (all included in the REG procedure of the SAS statistical software version 9.2, Cary, NC). We then reviewed the fit plots of the residual values over the independent variable by linear and polynomial regression to ensure that no significant residual association was present. Mathematical transformation of the dependent variable was only considered if the distribution of the normalized echocardiographic measurement suggested significant departure from the normal distribution (see below). We did not attempt to improve the goodness-of-fit by way of mathematical transformation of the dependent variable.

Preliminary analysis showed that the variance of the residual values was not homogenous across the entire range of body size for most dependent variable studied (ie, heteroscedasticity). We thus had to model variation of the standard deviation (SD) for the independent variable. We estimated the rate of increase of the SD by linear regression of the absolute value of the residual values against the independent variable. Because the residual values are assumed to be normally distributed, the absolute value of the residual values will adopt a half-normal distribution.[10] The mean of a half-standard normal distribution being $\sqrt{(2/\pi)}$, we estimated the SD using the predicted mean of the absolute value of the residual values multiplied by $\sqrt{(\pi/2)}$. *Z* scores were then calculated using equations listed in Table 1.

Assessment of the Validity of *Z* Scores

To assess if the newly computed *Z* scores were independent of growth, we plotted *Z* scores against weight, height, BSA, and age. We also verified the association with sex, resting heart rate (HR), and BMI adjusted for age and sex. At this stage, potential outliers were sought.

Downloaded from http://circimaging.ahajournals.org/ by guest on December 13, 2017

Table 1. Description Regression Models and *Z* Score Equations

Description	Equation for the Predicted Mean*	Equation for *Z* Score*
Linear	$y = c \times \mathrm{BSA} + d$	$Z = \frac{\mathrm{obs} - (c \times \mathrm{BSA} + d)}{g \times \mathrm{BSA} + h}$
Log-linear	$\ln(y) = c\mathrm{BSA} + d$	$Z = \frac{\ln(\mathrm{obs}) - (c \times \mathrm{BSA} + d)}{g \times \mathrm{BSA} + h}$
Reciprocal of linear	$\frac{1}{y} = c\mathrm{BSA} + d$	$Z = \frac{(1/\mathrm{obs}) - (c \times \mathrm{BSA} + d)}{g \times \mathrm{BSA} + h}$
Polynomial (second order)	$y = b \times \mathrm{BSA}^2 + c \times \mathrm{BSA} + d$	$Z = \frac{\mathrm{obs} - (b \times \mathrm{BSA}^2 + c \times \mathrm{BSA} + d)}{g \times \mathrm{BSA} + h}$
Reciprocal of polynomial (second order)	$\frac{1}{y} = b \times \mathrm{BSA}^2 + c \times \mathrm{BSA} + d$	$Z = \frac{(1/\mathrm{obs}) - (b \times \mathrm{BSA}^2 + c \times \mathrm{BSA} + d)}{g \times \mathrm{BSA} + h}$
Polynomial (third order)	$y = a \times \mathrm{BSA}^3 + b \times \mathrm{BSA}^2 + c \times \mathrm{BSA} + d$	$Z = \frac{\mathrm{obs} - (a \times \mathrm{BSA}^3 + b \times \mathrm{BSA}^2 + c \times \mathrm{BSA} + d)}{g \times \mathrm{BSA} + h}$
Allometric	$y = e \times \mathrm{BSA}^f$	$Z = \frac{\mathrm{obs} - (e \times \mathrm{BSA}^f)}{g \times \mathrm{BSA} + h}$
Log-allometric	$\ln(y) = e\mathrm{BSA}^f$	$Z = \frac{\ln(\mathrm{obs}) - (e \times \mathrm{BSA}^f)}{g \times \mathrm{BSA} + h}$

*The values for parameters *a* to *f* (predicted mean) and for parameters *g* and *h* (predicted SD) are listed in Tables 3 and 4. BSA indicates body surface area; obs, observation (measured echocardiographic parameter).

When potential outliers were identified, data entry and echocardiography cine-loops were reviewed, and corrections were made if needed. Any specific echocardiography measurement >3.5 SDs above or below the mean was then deleted and the *Z* scores were recomputed.

Z scores need to have a normal distribution to validly estimate percentiles. We evaluated *Z* scores for departure from a normal distribution with an expected mean of 0 and a SD of 1 by visual assessment (distribution histograms, box plots, and normal probability plots) and by using the Shapiro–Wilk statistic. This was done in all subjects, and for 3 subgroups corresponding to the lower, middle and highest tertiles of the independent variable. When *Z* scores adopted a log–normal distribution, the fitting process was started over using a log-transformed dependent variable. Log-transformed dependent variables were only used when the derived *Z* score showed less departure to a normal distribution compared with that of the dependent variable without log-transformation. In this article, model with log-transformed values are termed log-linear [$\ln(y)=ax+b$] and log-allometric [$\ln(y)=ax^b$] where appropriate. Similarly, some normalized dependent variable conformed to an inverse distribution. The reciprocal of the dependent variable ($1/y$) was then tested to seek improvement of the *Z* score distribution. In this article, such models are termed reciprocal of linear [$(1/y)=ax+b$]. All regression and *Z* score equations are listed in Table 1.

Statistical Analysis

We used SAS for Windows version 9.3 for all analyses (SAS Institute Inc, Cary, NC). We used the NLIN procedure for allometric regression and the GENMOD procedure for other regression models. Mean *Z* scores were compared using Student *t* test. The *t*-statistic was used to estimate *P* values for residual association. Departure from a normal distribution was evaluated by the Shapiro–Wilk statistic. A *P* value <0.05 was considered statistically significant.

Table 2. Subjects Characteristics

Characteristics	Median (Interquartile Range) or Number (%)	Range
Sex (male)	112 (48.1)	…
Age, y	12.1 (8.9)	1.3 to 18.0
Height, cm	151 (49)	77 to 186
Weight, kg	40.9 (34.6)	8.7 to 92
Body surface area, m^2	1.3 (0.8)	0.43 to 2.2
Body mass index, kg/m^2	17.8 (4.7)	13.4 to 27.8
Body mass index *Z* score	0.27 (1.42)	−1.9 to 1.9

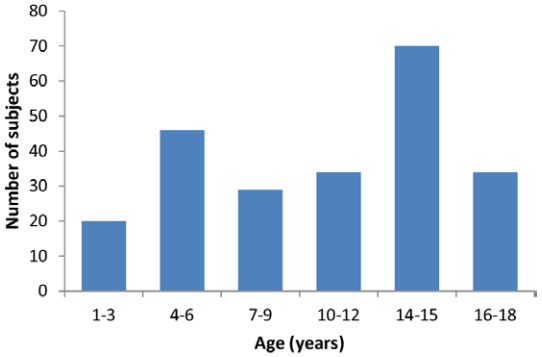


Figure 1. Subjects' age distribution.

Downloaded from http://circimaging.ahajournals.org/ by guest on December 13, 2017

Table 3. Models and Parameters for Pulse Wave Doppler and Related Measurements

Echo Measurements	n	Model	Predicted Mean Parameters						Predicted SD Parameters	
			a	*b*	*c*	*d*	*e*	*f*	*g*	*h*
Mitral valve E velocity, cm/s	232	Polynomial (third order)	5.363	−16.239	0.728	116.202	…	…	3.038	11.166
Mitral valve A velocity, cm/s	231	Log-allometric	…	…	…	…	3.873	−0.1115	0.038	0.199
Mitral valve E/A ratio	230	Log-allometric	…	…	…	…	0.770	0.3015	0.028	0.234
Mitral valve A wave duration, ms	227	Log-linear	…	…	0.154	4.492	…	…	−0.068	0.248
Mitral E wave deceleration time, ms	230	Log-linear	…	…	0.181	4.714	…	…	−0.032	0.170
Mitral valve closure to mitral valve opening time, ms	232	Allometric	…	…	…	…	371.692	0.1560	8.487	19.271
Isovolumic relaxation time, ms	230	Allometric	…	…	…	…	66.276	0.2416	0.056	7.143
Aortic left ventricular ejection time, ms	232	Allometric	…	…	…	…	283.430	0.1782	9.558	11.495
Left ventricular myocardial performance index	232	Allometric	…	…	…	…	0.318	−0.1184	−0.011	0.105
Pulmonary vein systolic velocity, cm/s	230	Log-linear	…	…	−0.144	3.966	…	…	0.043	0.198
Pulmonary vein diastolic velocity, cm/s	229	Allometric	…	…	…	…	61.079	0.0383	0.091	10.779
Pulmonary vein A wave velocity, cm/s	127	Log-linear	…	…	−0.152	3.065	…	…	0.000	0.260
Pulmonary vein A wave duration, ms	129	Allometric	…	…	…	…	86.719	0.4005	−1.491	20.477

Results

A total of 253 subjects was included in the study. One was excluded because of several outlier measurements, and 19 were excluded because of abnormal BMI-for-age *Z* scores (>2.0 or < −2.0), leaving 233 subjects for final analysis. Out of 5990 measurements available for analysis, 33 (0.55%) were considered outliers. These measurements were deleted from the database but the subjects were not excluded from the final analyses for the remaining measurements. Table 2 presents descriptive statistics for the participants included in the final analysis. Figure 1 shows our cohort's age distribution.

Model descriptions and parameters for PWD measurements and TDI measurements are shown in Tables 3 and 4, respectively. Corresponding equations are included in Table 1.

Table 4. Models and Parameters for Tissue Doppler Imaging Measurements

Echo Measurements	n	Model	Predicted Mean Parameters						Predicted SD Parameters	
			a	*b*	*c*	*d*	*e*	*f*	*g*	*h*
Pulse tissue mitral valve E velocity, cm/s	231	Polynomial (third order)	7.343	−31.380	42.148	1.463	…	…	−0.500	3.071
Pulse tissue mitral valve A velocity, cm/s	229	Log-linear	…	…	−0.029	1.831	…	…	0.044	0.179
Pulse tissue mitral valve S velocity, cm/s	231	Polynomial (third order)	4.631	−18.272	24.964	−1.064	…	…	0.163	1.605
Mitral valve E/E′ ratio	229	Allometric	…	…	…	…	5.724	−0.208	−0.197	1.227
Pulse tissue septal E velocity, cm/s	232	Polynomial (third order)	2.506	−11.701	17.341	7.290	…	…	0.141	2.014
Pulse tissue septal A velocity, cm/s	229	Log-linear	…	…	−0.031	1.827	…	…	0.047	0.142
Pulse tissue septal S velocity, cm/s	231	Polynomial (third order)	2.004	−7.375	8.982	4.856	…	…	0.028	0.840
Mitral valve E/septal E′ ratio	232	Allometric	…	…	…	…	7.234	−0.241	−0.068	1.332
Color tissue mitral valve E velocity, cm/s	227	Polynomial (third order)	2.400	−11.737	19.007	4.094	…	…	−0.118	2.471
Color tissue mitral valve A velocity, cm/s	224	Log-linear	…	…	0.165	0.850	…	…	0.014	0.432
Color tissue mitral valve S velocity, cm/s	227	Polynomial (third order)	3.587	−14.450	20.619	−2.772	…	…	0.727	0.733
Color tissue septal E velocity, cm/s	225	Polynomial (third order)	2.175	−10.532	16.084	3.761	…	…	0.556	0.819
Color tissue septal A velocity, cm/s	226	Allometric	…	…	…	…	3.894	−0.034	0.091	1.195
Color tissue septal S velocity, cm/s	226	Polynomial (third order)	2.372	−9.259	11.733	1.488	…	…	0.185	0.663

Downloaded from http://circimaging.ahajournals.org/ by guest on December 13, 2017

Table 5. Residual Association for Pulse Wave Doppler Measurements

	Residual Association									
	BSA		Age		HR		BMI		Sex	
Echo Measurements	Slope	*P* Value	Slope	*P* Value	Slope	*P* Value	Slope	*P* Value	Mean Difference	*P* Value
Mitral valve E velocity	0.000	1.00	−0.008	0.56	−0.001	0.86	0.103	0.17	−0.40	0.003
Mitral valve A velocity	0.048	0.76	−0.006	0.66	0.019	<0.001	0.103	0.16	0.01	0.96
Mitral valve E/A ratio	−0.010	0.95	0.003	0.84	−0.019	<0.001	−0.019	0.80	−0.19	0.16
Mitral valve A wave duration	−0.028	0.86	0.006	0.67	−0.015	<0.001	−0.024	0.75	−0.01	0.95
Mitral valve deceleration time	−0.033	0.83	0.007	0.62	−0.017	<0.001	−0.079	0.29	−0.14	0.30
Mitral valve closure to mitral valve opening time	0.004	0.98	0.017	0.24	−0.023	<0.001	−0.173	0.02	0.02	0.87
Isovolumic relaxation time	−0.006	0.97	0.008	0.55	−0.012	0.004	−0.133	0.07	0.01	0.93
Aortic left ventricular ejection time	0.025	0.87	0.012	0.38	−0.027	<0.001	−0.153	0.04	0.22	0.09
Left ventricular myocardial performance index	0.004	0.98	0.005	0.73	0.004	0.32	−0.012	0.87	−0.20	0.13
Pulmonary vein systolic velocity	−0.003	0.96	−0.009	0.53	−0.002	0.66	0.206	0.004	0.25	0.05
Pulmonary vein diastolic velocity	−0.012	0.94	−0.008	0.56	−0.005	0.19	0.056	0.44	−0.16	0.22
Pulmonary vein A wave velocity	0.000	1.00	−0.008	0.69	0.002	0.80	0.046	0.65	−0.21	0.25
Pulmonary vein A wave duration	0.002	0.99	−0.002	0.95	−0.008	0.30	−0.097	0.41	−0.44	0.04

BMI indicates body mass index; BSA, body surface area; and HR, heart rate.

Residual associations are shown in Tables 5 and 6 for PWD measurements and TDI measurements, respectively. *Z* scores may be estimated by calculating the predicted mean and predicted SD using the parameters in Tables 3 and 4 with the equations from Table 1 for the corresponding model. Scatter plots with predicted *Z* score boundaries of each measurement are available in the Data Supplement.

Choice of BSA as the Independent Variable

Preliminary analyses indicated that for most measurements, *Z* scores adjusted for BSA had less residual association with age, height and weight, compared with *Z* scores adjusted for age, height or weight. Numerous trials were undertaken to seek improved normalization with weight or height compared with BSA. For measurements with strong associations with growth, weight performed better in children aged <2 years while the height was superior in adolescents. That being said, when the entire growth range was considered, BSA was overall superior to adjust for growth and created less distortion in small children or tall adolescents compared with weight or height alone (data not shown). We therefore only present *Z* scores adjusted for BSA. Using one normalizing variable for

Table 6. Residual Association for Tissue Doppler Imaging Measurements

	Residual Association									
	BSA		Age		HR		BMI		Sex	
Echo Measurements	Slope	*P* Value	Slope	*P* Value	Slope	*P* Value	Slope	*P* Value	Mean Difference	*P* Value
Pulse tissue mitral valve E velocity	0.000	1.00	−0.002	0.87	−0.004	0.37	−0.016	0.83	0.13	0.33
Pulse tissue mitral valve A velocity	−0.027	0.87	−0.009	0.53	0.013	0.001	0.083	0.26	0.03	0.84
Pulse tissue mitral valve S velocity	0.000	1.00	−0.001	0.97	0.005	0.21	−0.161	0.03	0.00	1.00
Mitral valve E/E′ ratio	0.122	0.43	0.004	0.77	0.002	0.57	0.075	0.30	−0.41	0.002
Pulse tissue septal E velocity	0.000	1.00	0.004	0.79	0.000	1.00	−0.091	0.20	0.12	0.35
Pulse tissue septal A velocity	−0.041	0.79	−0.015	0.28	0.015	<0.001	0.146	0.04	−0.13	0.34
Pulse tissue septal S velocity	0.000	1.00	−0.010	0.45	0.010	0.011	0.177	0.02	−0.19	0.15
Mitral valve E/septal E′ ratio	0.064	0.69	−0.007	0.63	−0.001	0.89	0.171	0.02	−0.45	<0.001
Color tissue mitral valve E velocity	0.000	1.00	0.000	0.98	−0.007	0.11	−0.055	0.45	0.15	0.27
Color tissue mitral valve A velocity	−0.003	0.99	−0.008	0.59	0.009	0.05	0.063	0.40	−0.09	0.53
Color tissue mitral valve S velocity	−0.001	1.00	0.003	0.84	0.000	0.97	−0.139	0.06	0.04	0.77
Color tissue septal E velocity	0.000	1.00	−0.002	0.88	−0.003	0.44	−0.086	0.24	0.10	0.46
Color tissue septal A velocity	0.058	0.72	−0.003	0.84	0.007	0.12	0.059	0.43	−0.23	0.10
Color tissue septal S velocity	0.000	1.00	−0.010	0.51	0.006	0.14	0.059	0.43	−0.19	0.15

BMI indicates body mass index; BSA, body surface area; and HR, heart rate.

Downloaded from http://circimaging.ahajournals.org/ by guest on December 13, 2017

young children and another for adolescents would have created breaks in the centile lines at the point of transition from one equation to the other.

PWD Measurements

Normalization for body size was successful for all PWD measurements with adequate distribution of *Z* scores and little residual association with body size. Figure 2 shows scatter plots of selected PWD velocity measurements with predicted *Z* score boundaries. Scatter plots and Z score boundaries for all PWD measurements are available in the Data Supplement. As an example, Figure 3 shows absence of residual association with BSA and lack of significant departure from a normal distribution for mitral valve E-wave velocity. However, several measurements known to have a dependency to HR had *Z* scores with significant residual association with HR. All PWD measurements *Z* scores related to mitral valve were still dependent on HR after normalization, except for mitral E-wave velocity. The same was observed for isovolumetric relaxation time. For example, the residual slope of the *Z* score for mitral valve A-wave duration versus HR was −0.019 (Table 5; Figure 4) meaning a reduction of close to 0.2 SD of A-wave duration for each 10 beats per minute increase of resting HR. While this association is expected, such strong residual association indicates that the use of *Z* scores may potentially be biased for these measurements.

TDI Measurements

Because TDI velocities are not equivalent when estimated using PWD (peak velocities) and color Doppler (mean velocities) techniques, they are presented separately. Scatter plots of mitral valve lateral pulse wave tissue velocity measurements and *Z* score boundaries according to the BSA are shown in Figure 5. Scatter plots and Z score boundaries for all TDI measurements

Downloaded from http://circimaging.ahajournals.org/ by guest on December 13, 2017

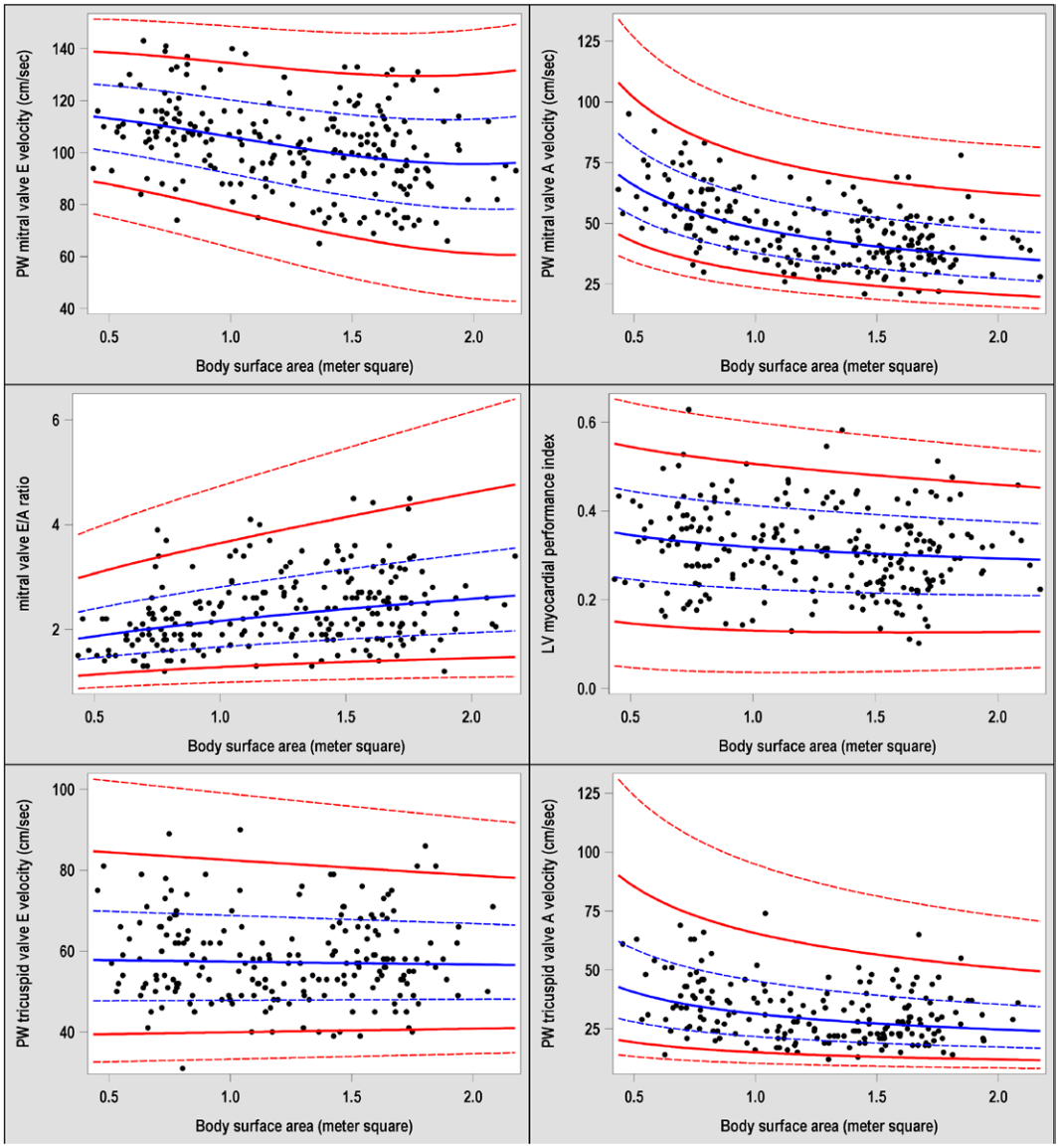


Figure 2. Scatter plot of selected pulse wave Doppler velocity measurements according to body surface area with predicted *Z* score boundaries. Solid blue line, *Z*=0; dashed blue lines, *Z*=1 and −1; solid red lines, *Z*=2 and −2; dashed red lines, *Z*=3 and −3. LV indicates left ventricle; and PW, pulse wave.

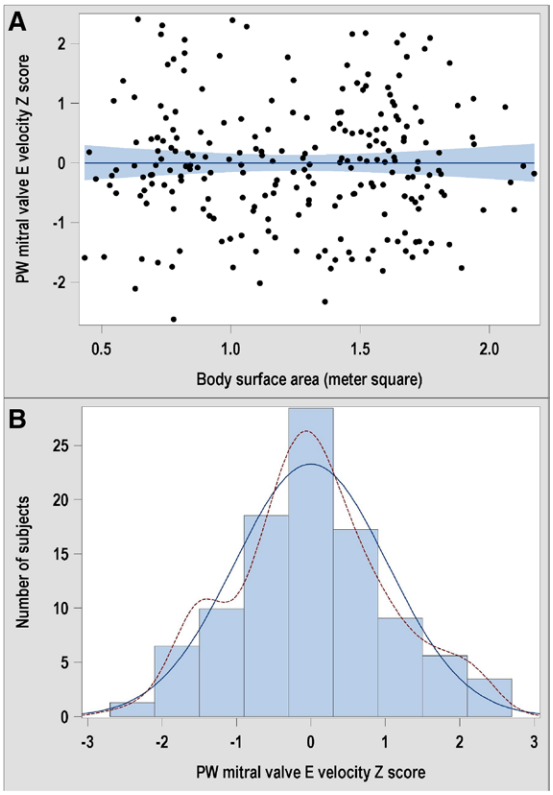


Figure 3. Absence of residual association with body surface area (**A**) and lack of significant departure from a normal distribution (**B**) for mitral valve E-wave velocity *Z* score.

are available in the Data Supplement. TDI E- and S-waves adopted a third order polynomial pattern where velocities in young children were lowest, reached a plateau for school-aged children and then increased again in older children. A-waves were less dependent on growth and most required log-transformation so that *Z* scores conformed to a normal distribution.

Similar to PWD measurements, residual association with HR was found for some TDI measurements (mostly A-wave velocities). This was less pronounced for velocities estimated by the color Doppler technique compared with that of the pulse Doppler technique. The magnitude of residual association with HR was overall lower compared to that of the PWD measurements.

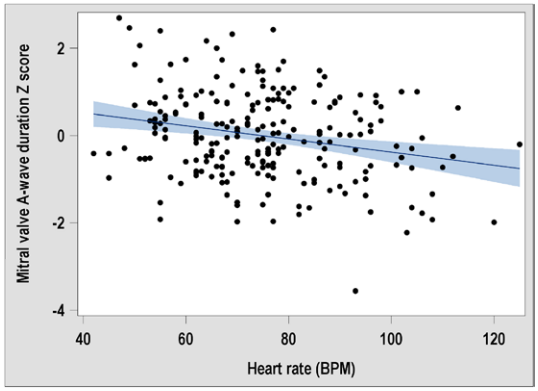


Figure 4. Mitral valve A-wave duration *Z* score residual association with resting heart rate.

Effect of Sex and BMI-for-Age

Most *Z* scores were independent of sex, except for pulmonary vein A-wave duration, mitral valve E-wave velocity, and, consequently, mitral E/E′ ratio. Although statistically significant, we think that these associations with sex were the result of chance alone, because most other parameters were not significantly influenced by sex once adjusted for BSA. We also observed a mild degree of residual association between BMI-for-age and PWD and TDI velocities. Such a residual association was mostly present in measurements with a stronger relationship with body size (see Discussion).

Discussion

In this study, we present *Z* score equations for most left-sided PWD and TDI velocities used in pediatric echocardiography. These equations were computed from a prospectively recruited cohort of healthy pediatric participants. We identified significant heteroscedasticity and nonlinear association with BSA for many measurements and a standardized approach was used to optimize regression modeling to produce *Z* scores with adequate data distribution and little residual association with body size. We also identified several measurements with significant residual association with HR despite normalization.

Recently, Cantinotti and Lopez[3] reviewed currently available nomograms and reference values for PWD and TDI velocities in pediatric echocardiography. They rightfully concluded that echocardiographic and normalization methodologies were heterogeneous, inconsistent and often incomplete. Of the many available nomograms, 12 studies were performed on >100 participants.[1,2,11–20] Most of them, but not all,[11,15,16,20] have reported an association with Doppler velocities and growth or age. Despite the nonlinear relationship between most Doppler velocities and age, most authors have so far relied on simple linear regression to express predicted mean velocities or *Z* scores.[2,11–14,17,18] Furthermore, although we observed significant heteroscedasticity for most measured parameters, we found no studies where the SD was modeled or weighed to adjust for its variation according to growth. When these 2 important aspects are unaccounted for, one could expect normalized measurements or *Z* scores with significant residual heteroscedasticity or residual association growth. Both could lead to significantly underestimate or overestimated *Z* scores.

Similar to what was observed several times previously,[3] many PWD and TDI velocities had residual association with HR despite adjustment for BSA. Despite all efforts to standardize echocardiographic functional measurements, physiological variation of HR may have a significant influence on some of them and may affect their reproducibility. Because of the complex interactions between HR, growth and blood flow on tissue dynamics, we did not attempt to include HR in our mathematical models. Nevertheless, we elected to propose *Z* score equations even when a residual association with HR was detected. Although these *Z* scores may well be influenced by HR, we think that they still offer the benefit of being adjusted for body size. With that in mind, normalized measurements with HR dependency should be interpreted with caution, especially in individuals with resting HR unusually low or high for their age.

Downloaded from http://circimaging.ahajournals.org/ by guest on December 13, 2017

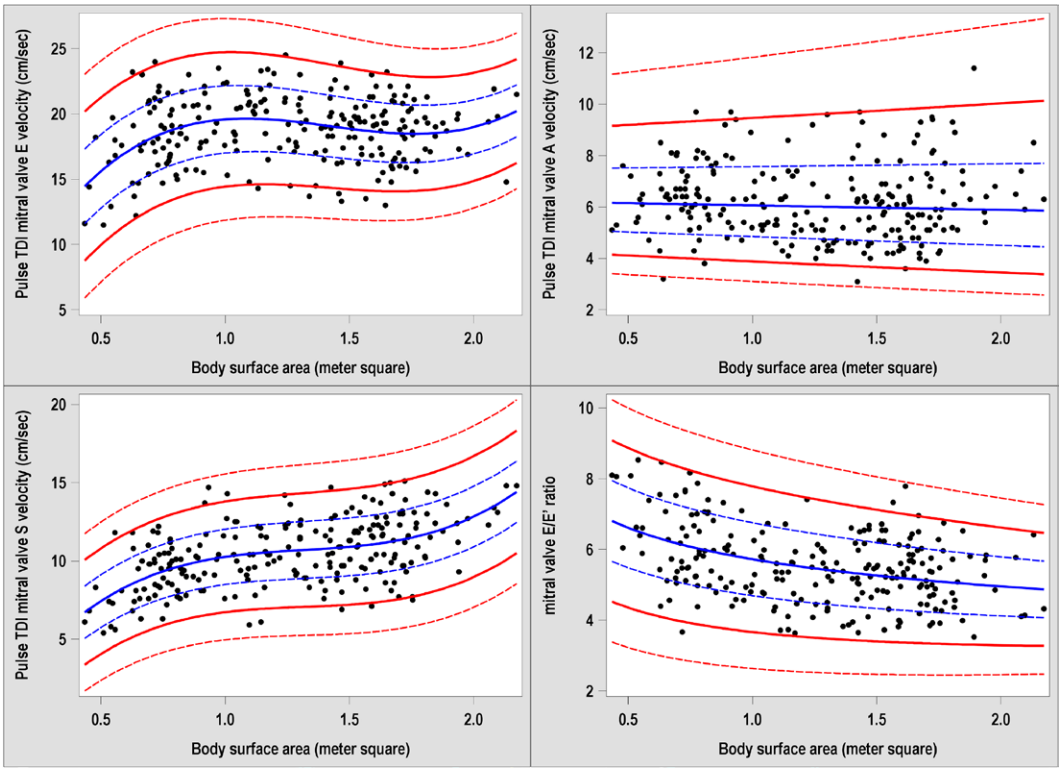


Figure 5. Scatter plot of selected tissue Doppler imaging velocity measurements according to body surface area with predicted *Z* score boundaries. Solid blue line, *Z*=0; dashed blue lines, *Z*=1 and −1; solid red lines, *Z*=2 and −2; dashed red lines, *Z*=3 and −3.

In this study, we used parametric modeling to propose reference values and *Z* score equations. Other methodologies exist to estimate reference centiles of a normal population. These include the LMS method and quantile regression.[21,22] Both of these approaches have the benefit of being less stringent in the distribution assumptions. Despite this, we used parametric modeling because of the simplicity of its application (simple *Z* score equations instead of centile limit tables), and because we were confident that the measurements' distribution were close enough to the distributional assumptions so that no significant residual error was present. In the future, it would be interesting to use nonparametric methodologies as a validation tool for the current equations.

In this study, we excluded children younger than 1 year of age. Transitional circulation with decreasing pulmonary resistances as well as rapid growth in young babies has a major impact on most PWD and TDI measurements. Our preliminary results did not allow the construction of reliable *Z* scores for such young children, mostly because of insufficient sample size. We consequently elected to exclude them from this analysis.

We also excluded children with abnormal BMI for their age and sex. Despite this, we observed that some normalized Doppler velocities had a residual association with BMI. We have previously observed that normalization for BSA in pediatric echocardiography could introduce a bias related to the level of fat mass, mostly in adolescents.[23] While this effect is less likely to play an important role because of the weaker association of Doppler velocities with BSA, caution is required when any measurement is normalized for BSA for an obese patient. Also, few participants in our cohort had BSA>2 m^2. Small numbers at the end of the growth spectrum could cause some distortion in the model predictions and caution should be observed in individuals with BSA significantly above 2 m^2. Furthermore, even if the older adolescents in our cohort had reached adult size, one should not infer our results to an adult patient population.

Conclusions

In this study, we present *Z* scores for normalized PWD and TDI velocities in pediatric echocardiography. We are confident that we have successfully reduced the influence of body size in most Doppler velocities used in today's echocardiography laboratories. This will ease the interpretation of these parameters in pediatric echocardiography. As *Z* scores describe the normal limit of a healthy population, other studies are needed to further define the threshold above which health becomes a disease by integrating other important factors such as ventricular morphology, loading condition, and HR.

Acknowledgments

The authors wish to acknowledge the Fonds de Recherche Santé Québec for supporting the Centre de Recherche du Centre Hospitalier Universitaire de Sherbrooke; the Kidney Foundation of Canada, the Canadian Diabetes Association (KRESCENT Program Joint New Investigator Award), and Canadian Institutes of Health Research for scholarships and operating support to Dr Cherney; and the Banting and Best Diabetes Centre Graduate Studentship for a scholarship to R. Har.

Sources of Funding

This project was supported in part by the Labatt Family Heart Centre Innovations Fund and by operating grants from the Juvenile Diabetes

Downloaded from http://circimaging.ahajournals.org/ by guest on December 13, 2017

Research Foundation, Juvenile Diabetes Research Foundation–Canadian Clinical Trials Network.

Disclosures

None.

References

1. Schmitz L, Koch H, Bein G, Brockmeier K. Left ventricular diastolic function in infants, children, and adolescents. Reference values and analysis of morphologic and physiologic determinants of echocardiographic Doppler flow signals during growth and maturation. *J Am Coll Cardiol*. 1998;32:1441–1448.
2. Eidem BW, McMahon CJ, Cohen RR, Wu J, Finkelshteyn I, Kovalchin JP, Ayres NA, Bezold LI, O'Brian Smith E, Pignatelli RH. Impact of cardiac growth on Doppler tissue imaging velocities: a study in healthy children. *J Am Soc Echocardiogr*. 2004;17:212–221. doi: 10.1016/j.echo.2003.12.005.
3. Cantinotti M, Lopez L. Nomograms for blood flow and tissue Doppler velocities to evaluate diastolic function in children: a critical review. *J Am Soc Echocardiogr*. 2013;26:126–141. doi: 10.1016/j.echo.2012.11.017.
4. Colan SD. The why and how of Z scores. *J Am Soc Echocardiogr*. 2013;26:38–40. doi: 10.1016/j.echo.2012.11.005.
5. Mawad W, Drolet C, Dahdah N, Dallaire F. A review and critique of the statistical methods used to generate reference values in pediatric echocardiography. *J Am Soc Echocardiogr*. 2013;26:29–37. doi: 10.1016/j.echo.2012.09.021.
6. Haycock GB, Schwartz GJ, Wisotsky DH. Geometric method for measuring body surface area: a height-weight formula validated in infants, children, and adults. *J Pediatr*. 1978;93:62–66.
7. Sluysmans T, Colan SD. Theoretical and empirical derivation of cardiovascular allometric relationships in children. *J Appl Physiol (1985)*. 2005;99:445–457. doi: 10.1152/japplphysiol.01144.2004.
8. de Onis M, Garza C, Victora CG, Bhan MK, Norum KR. The WHO Multicentre Growth Reference Study (MGRS): rationale, planning, and implementation. *Food Nutr Bull*. 2004;25:S3–S84.
9. de Onis M, Onyango AW, Borghi E, Siyam A, Nishida C, Siekmann J. Development of a WHO growth reference for school-aged children and adolescents. *Bull World Health Organ*. 2007;85:660–667.
10. Altman DG. Construction of age-related reference centiles using absolute residuals. *Stat Med*. 1993;12:917–924.
11. Cui W, Roberson DA, Chen Z, Madronero LF, Cuneo BF. Systolic and diastolic time intervals measured from Doppler tissue imaging: normal values and Z-score tables, and effects of age, heart rate, and body surface area. *J Am Soc Echocardiogr*. 2008;21:361–370. doi: 10.1016/j.echo.2007.05.034.
12. Roberson DA, Cui W. Right ventricular Tei index in children: effect of method, age, body surface area, and heart rate. *J Am Soc Echocardiogr*. 2007;20:764–770. doi: 10.1016/j.echo.2006.11.002.
13. Roberson DA, Cui W, Chen Z, Madronero LF, Cuneo BF. Annular and septal Doppler tissue imaging in children: normal z-score tables and effects of age, heart rate, and body surface area. *J Am Soc Echocardiogr*. 2007;20:1276–1284. doi: 10.1016/j.echo.2007.02.023.
14. Harada K, Suzuki T, Tamura M, Ito T, Shimada K, Takada G. Effect of aging from infancy to childhood on flow velocity patterns of pulmonary vein by Doppler echocardiography. *Am J Cardiol*. 1996;77:221–224.
15. Ishii M, Eto G, Tei C, Tsutsumi T, Hashino K, Sugahara Y, Himeno W, Muta H, Furui J, Akagi T, Fukiyama R, Toyoda O, Kato H. Quantitation of the global right ventricular function in children with normal heart and congenital heart disease: a right ventricular myocardial performance index. *Pediatr Cardiol*. 2000;21:416–421.
16. Kapusta L, Thijssen JM, Cuypers MH, Peer PG, Daniëls O. Assessment of myocardial velocities in healthy children using tissue Doppler imaging. *Ultrasound Med Biol*. 2000;26:229–237.
17. Mori K, Hayabuchi Y, Kuroda Y, Nii M, Manabe T. Left ventricular wall motion velocities in healthy children measured by pulsed wave Doppler tissue echocardiography: normal values and relation to age and heart rate. *J Am Soc Echocardiogr*. 2000;13:1002–1011.
18. O'Leary PW, Durongpisitkul K, Cordes TM, Bailey KR, Hagler DJ, Tajik J, Seward JB. Diastolic ventricular function in children: a Doppler echocardiographic study establishing normal values and predictors of increased ventricular end-diastolic pressure. *Mayo Clin Proc*. 1998;73:616–628.
19. Rafeiyian S, Looti-Shahrokh B, Motamedi MR, Karkhaneh-Yousefi Z, Mojtahedzadeh S, Kouhi A. Pulse tissue Doppler analysis of tricuspid annular motion in Iranian children. *Int J Cardiovasc Imaging*. 2006;22:363–367. doi: 10.1007/s10554-005-9061-8.
20. Swaminathan S, Ferrer PL, Wolff GS, Gómez-Marín O, Rusconi PG. Usefulness of tissue Doppler echocardiography for evaluating ventricular function in children without heart disease. *Am J Cardiol*. 2003;91:570–574.
21. Wei Y, Pere A, Koenker R, He X. Quantile regression methods for reference growth charts. *Stat Med*. 2006;25:1369–1382. doi: 10.1002/sim.2271.
22. Cole TJ, Green PJ. Smoothing reference centile curves: the LMS method and penalized likelihood. *Stat Med*. 1992;11:1305–1319.
23. Dallaire F, Bigras JL, Prsa M, Dahdah N. Bias related to body mass index in pediatric echocardiographic z scores [published online ahead of print November 12, 2014]. *Pediatr Cardiol*. doi: 10.1007/s00246-014-1063-7. http://link.springer.com/article/10.1007%2Fs00246-014-1063-7. Accessed January 22, 2014.

CLINICAL PERSPECTIVE

In healthy children, blood flow and tissue velocities vary with body size. Echocardiographic measurements of pulse wave Doppler and tissue Doppler imaging velocities must therefore be adjusted for body size. In this study, we found that most pulse wave Doppler and tissue Doppler imaging velocities were associated with body surface area, often in a nonlinear fashion. We used parametric regression to normalize them according to body surface area. We therefore provide equations that allow the estimation of a *Z* score for most left-sided pulse wave Doppler and tissue Doppler imaging routinely used in clinical setting. The use of these *Z* scores should improve the clinical interpretation of pulse wave Doppler and tissue Doppler imaging velocities by removing the effect of body size.

Downloaded from http://circimaging.ahajournals.org/ by guest on December 13, 2017

Circulation
Cardiovascular Imaging

American Heart Association®

Reference Values for Pulse Wave Doppler and Tissue Doppler Imaging in Pediatric Echocardiography

Frederic Dallaire, Cameron Slorach, Wei Hui, Taisto Sarkola, Mark K. Friedberg, Timothy J. Bradley, Edgar Jaeggi, Andreea Dragulescu, Ronnie L.H. Har, David Z.I. Cherney and Luc Mertens

Circ Cardiovasc Imaging. 2015;8:
doi: 10.1161/CIRCIMAGING.114.002167
Circulation: Cardiovascular Imaging is published by the American Heart Association, 7272 Greenville Avenue, Dallas, TX 75231
Copyright © 2015 American Heart Association, Inc. All rights reserved.
Print ISSN: 1941-9651. Online ISSN: 1942-0080

The online version of this article, along with updated information and services, is located on the World Wide Web at:
http://circimaging.ahajournals.org/content/8/2/e002167

Data Supplement (unedited) at:
http://circimaging.ahajournals.org/content/suppl/2015/01/28/CIRCIMAGING.114.002167.DC1

Permissions: Requests for permissions to reproduce figures, tables, or portions of articles originally published in *Circulation: Cardiovascular Imaging* can be obtained via RightsLink, a service of the Copyright Clearance Center, not the Editorial Office. Once the online version of the published article for which permission is being requested is located, click Request Permissions in the middle column of the Web page under Services. Further information about this process is available in the Permissions and Rights Question and Answer document.

Reprints: Information about reprints can be found online at:
http://www.lww.com/reprints

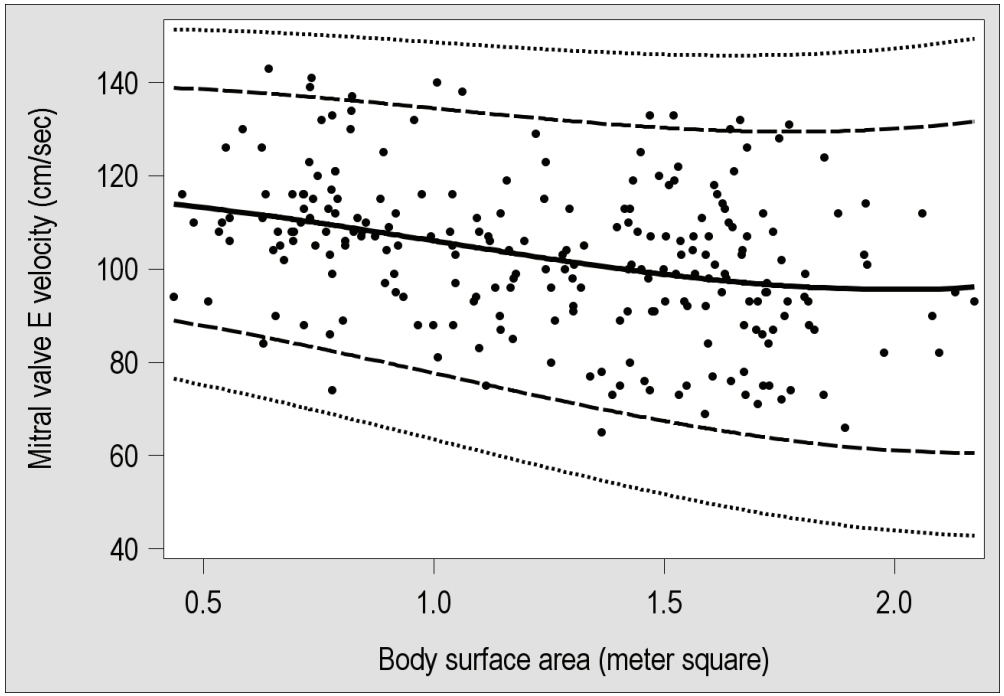
Subscriptions: Information about subscribing to *Circulation: Cardiovascular Imaging* is online at:
http://circimaging.ahajournals.org//subscriptions/

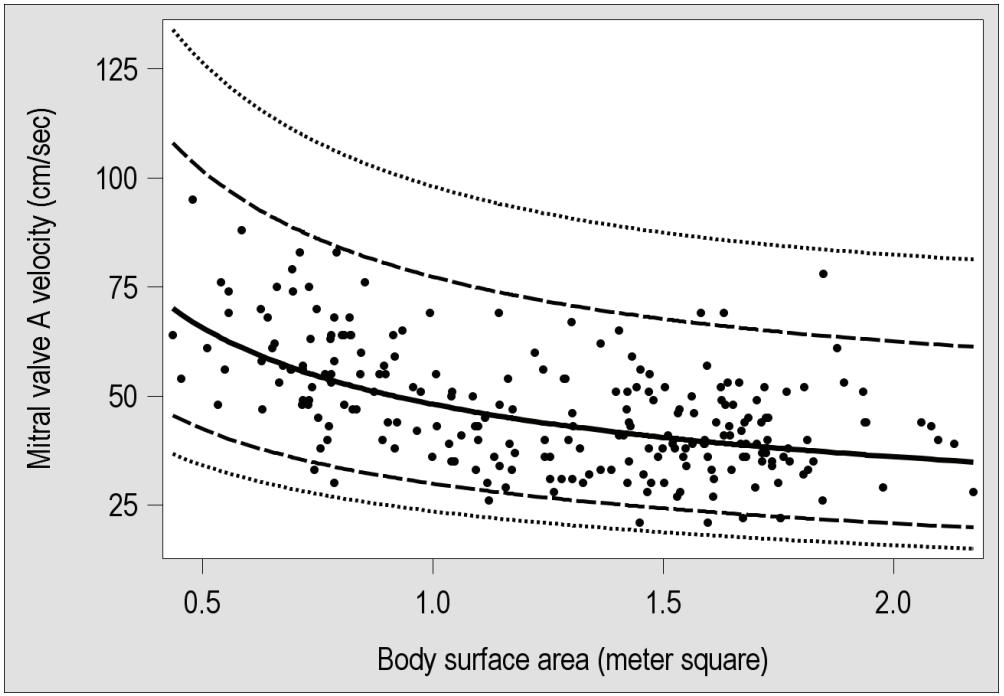
Downloaded from http://circimaging.ahajournals.org/ by guest on December 13, 2017

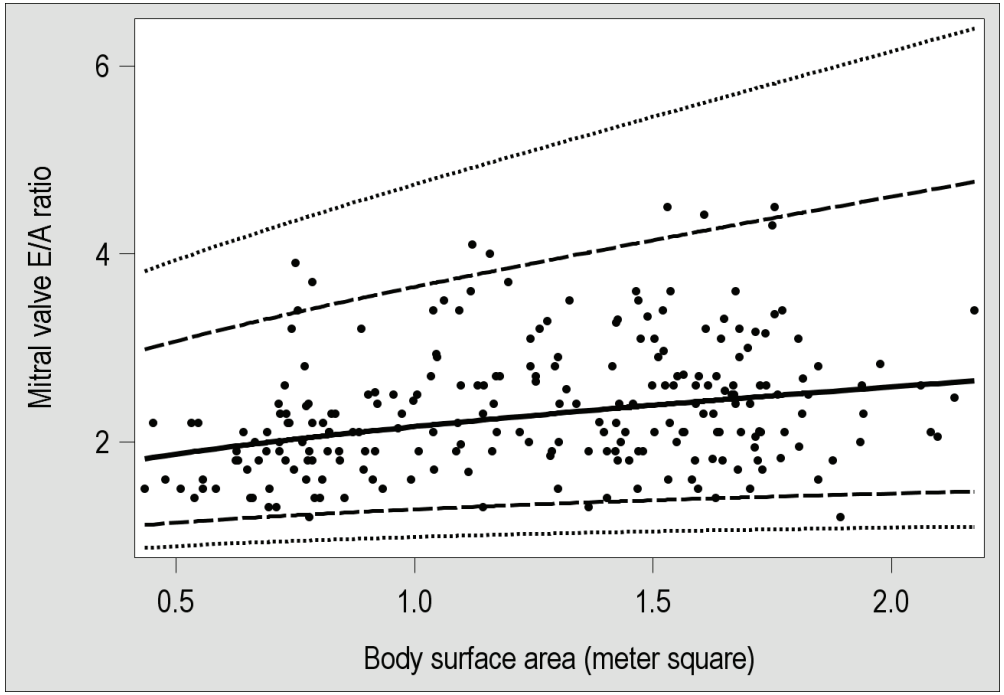
Online supplement

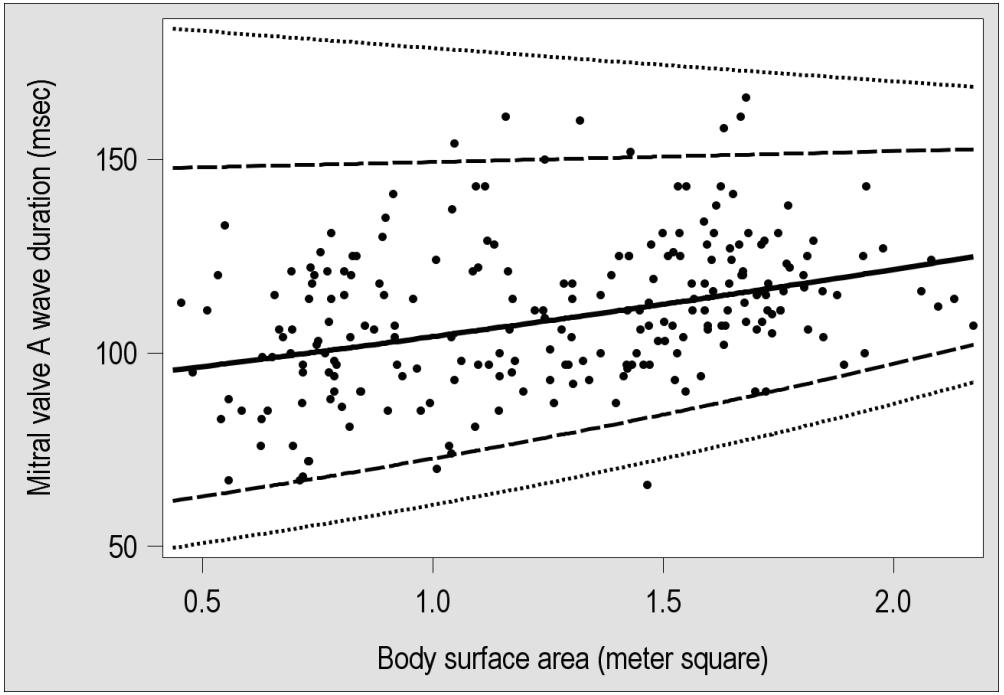
Dallaire *et al*. - Reference values for pulse wave Doppler and tissue Doppler imaging in pediatric echocardiography.

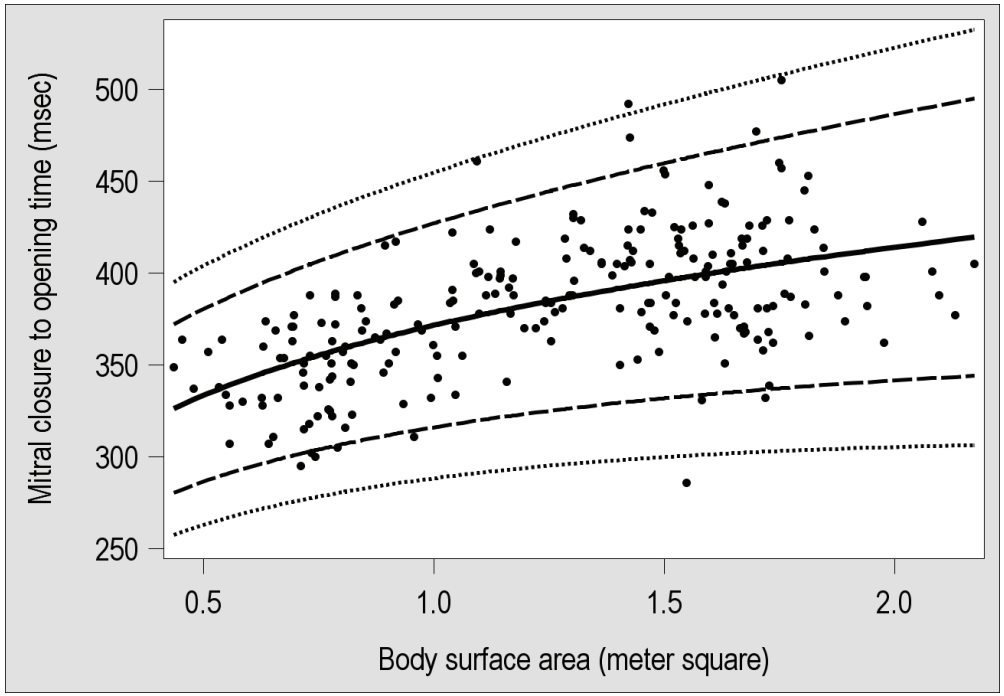
Scatter plots of all measurements with Z score boundaries according to BSA. Solid blue line: Z = 0; long dash lines: Z = 2 and −2; short dash lines: Z = 3 and −3.

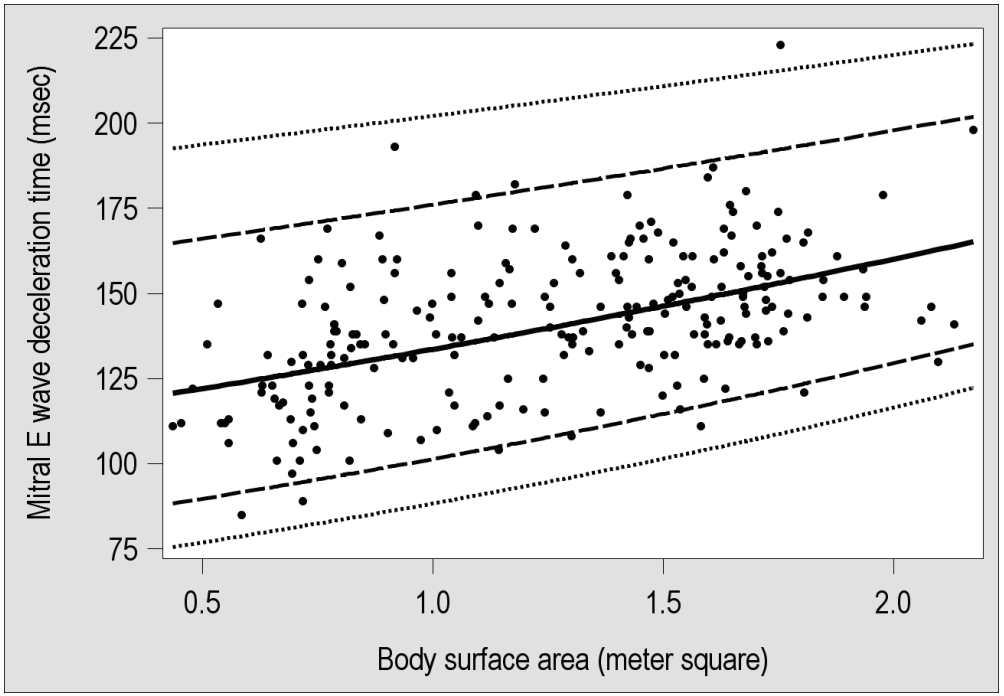

Mitral valve E velocity (cm/sec)
140
120
100
80
60
40
0.5
1.0
1.5
2.0
Body surface area (meter square)

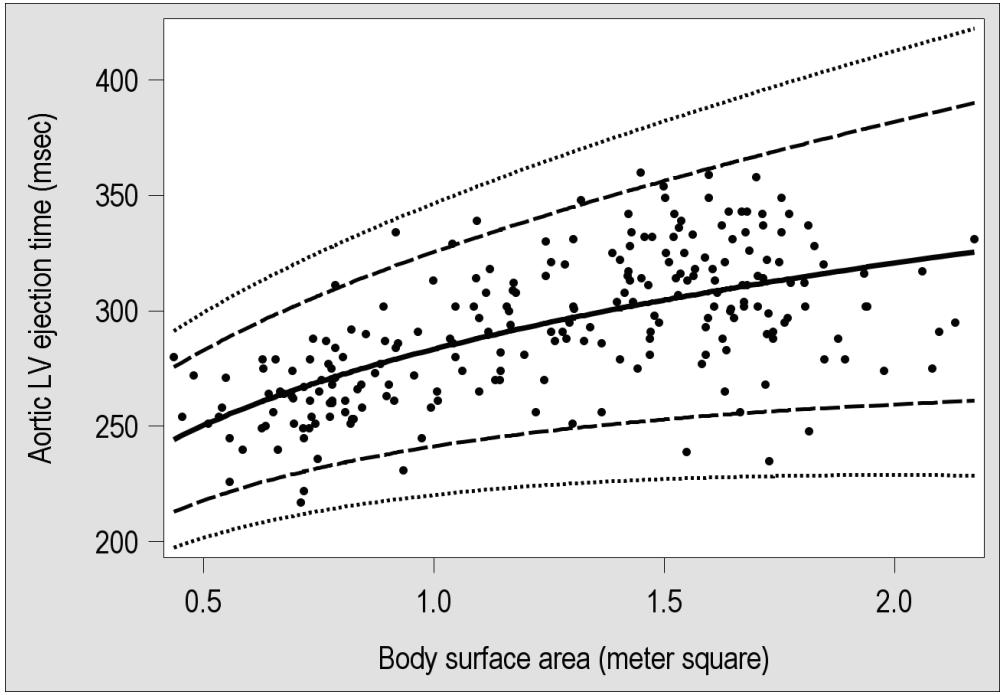

Mitral valve A velocity (cm/sec)
125
100
75
50
25
0.5
1.0
1.5
2.0
Body surface area (meter square)

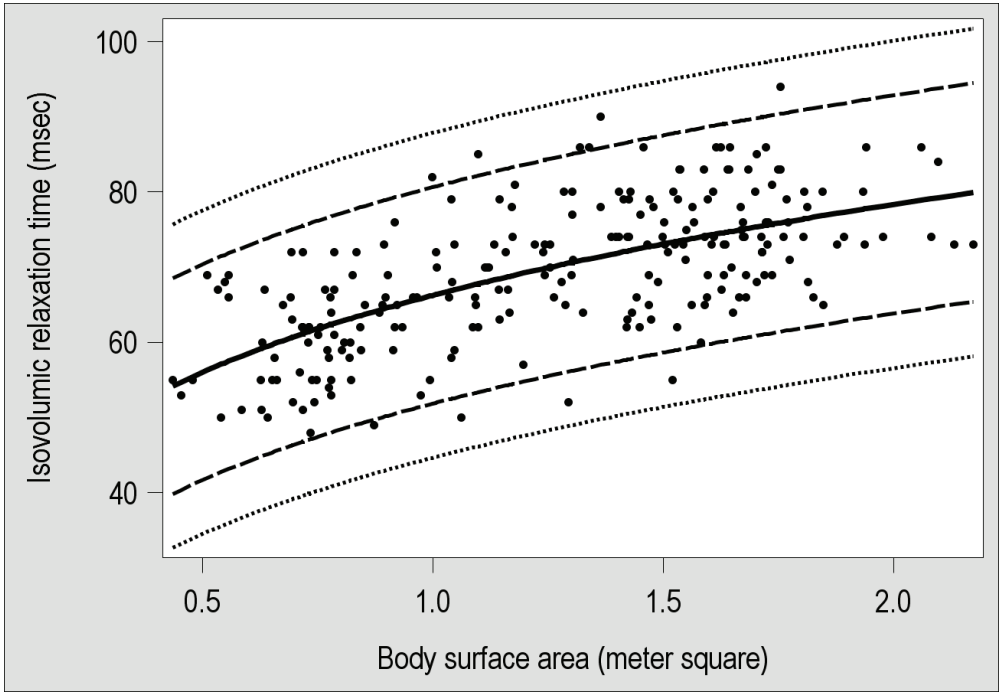

Mitral valve E/A ratio
6
4
2
0.5
1.0
1.5
2.0
Body surface area (meter square)

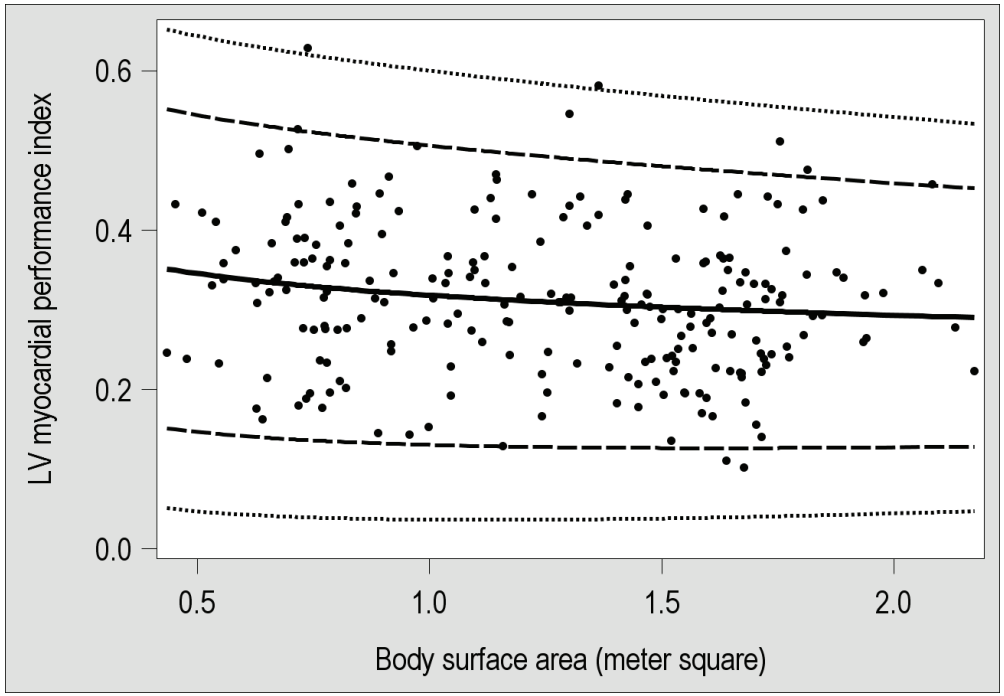

Mitral valve A wave duration (msec)
150
100
50
0.5
1.0
1.5
2.0
Body surface area (meter square)

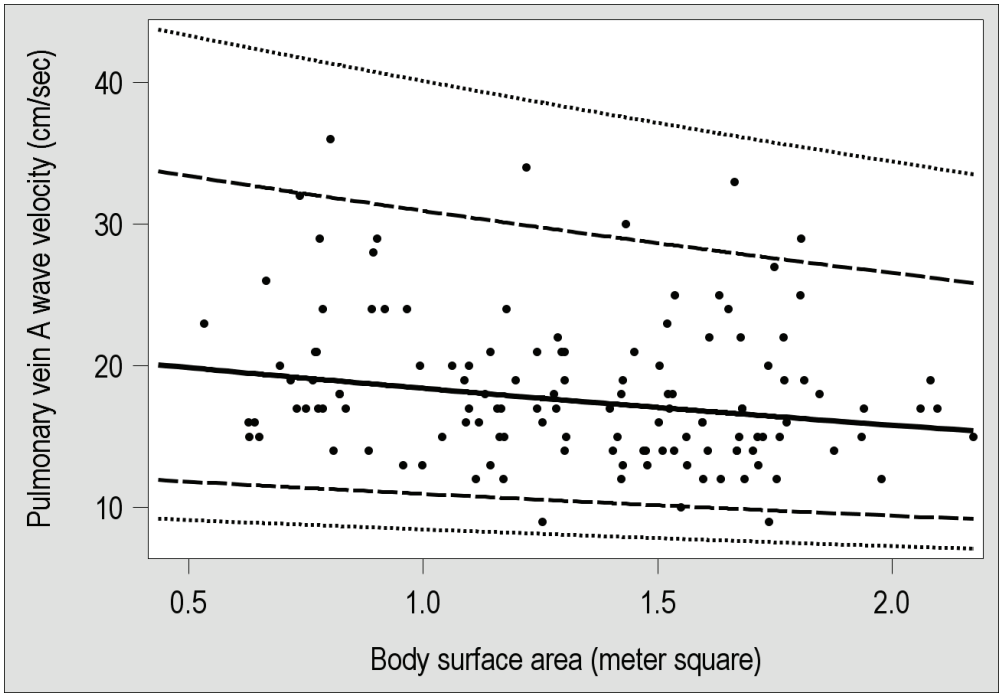

Mitral closure to opening time (msec)
500
450
400
350
300
250
0.5
1.0
1.5
2.0
Body surface area (meter square)

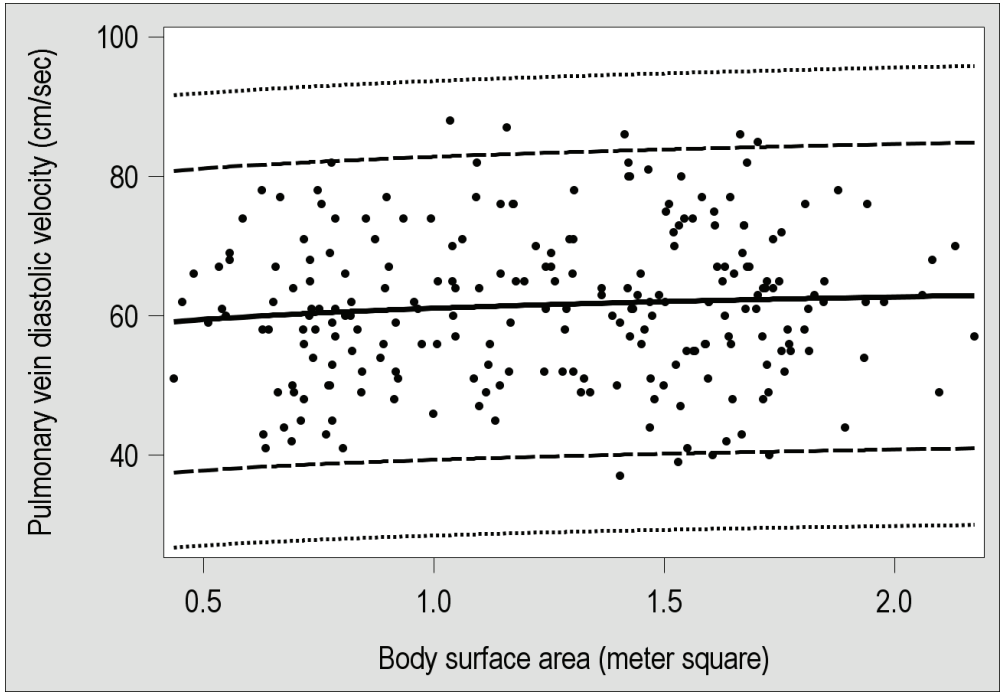

Mitral E wave deceleration time (msec)
225
200
175
150
125
100
75
0.5
1.0
1.5
2.0
Body surface area (meter square)

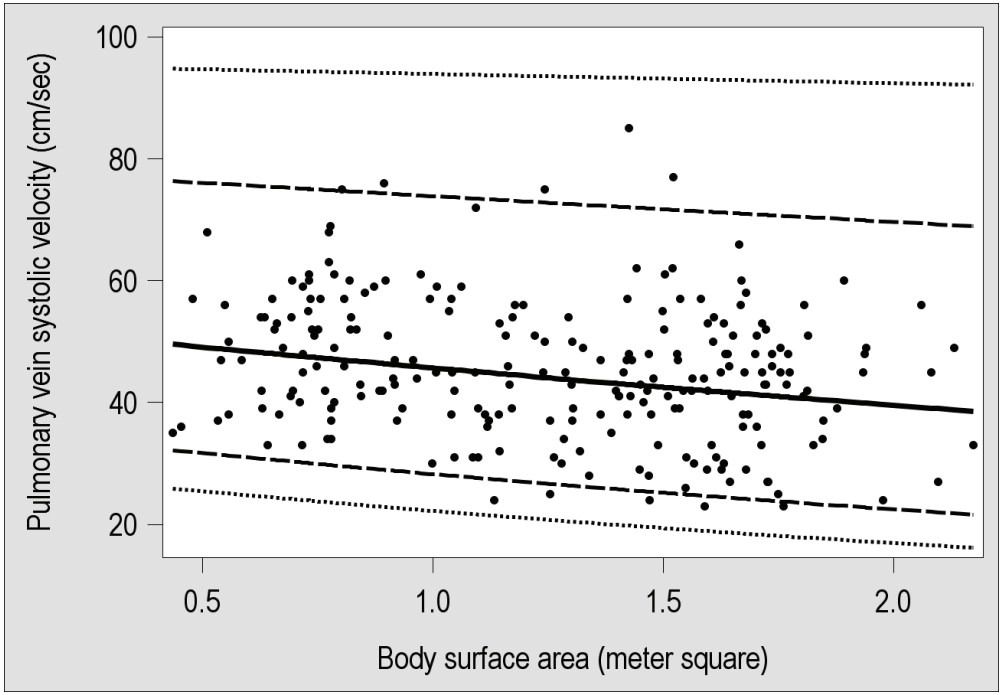

Aortic LV ejection time (msec)
400
350
300
250
200
0.5
1.0
1.5
2.0
Body surface area (meter square)

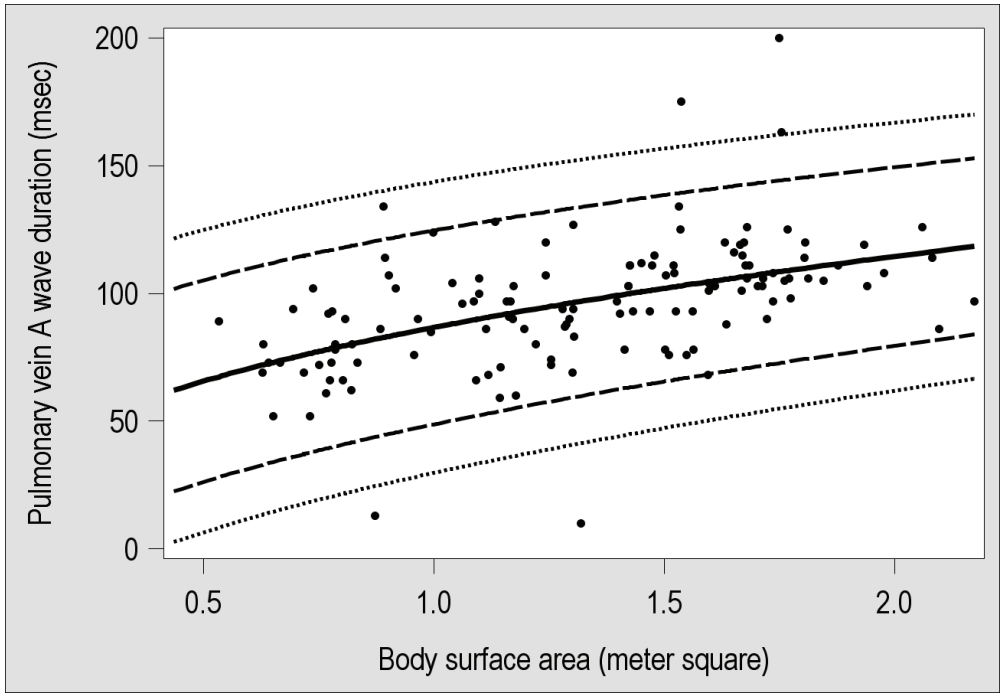

Isovolumic relaxation time (msec)
100
80
60
40
0.5
1.0
1.5
2.0
Body surface area (meter square)

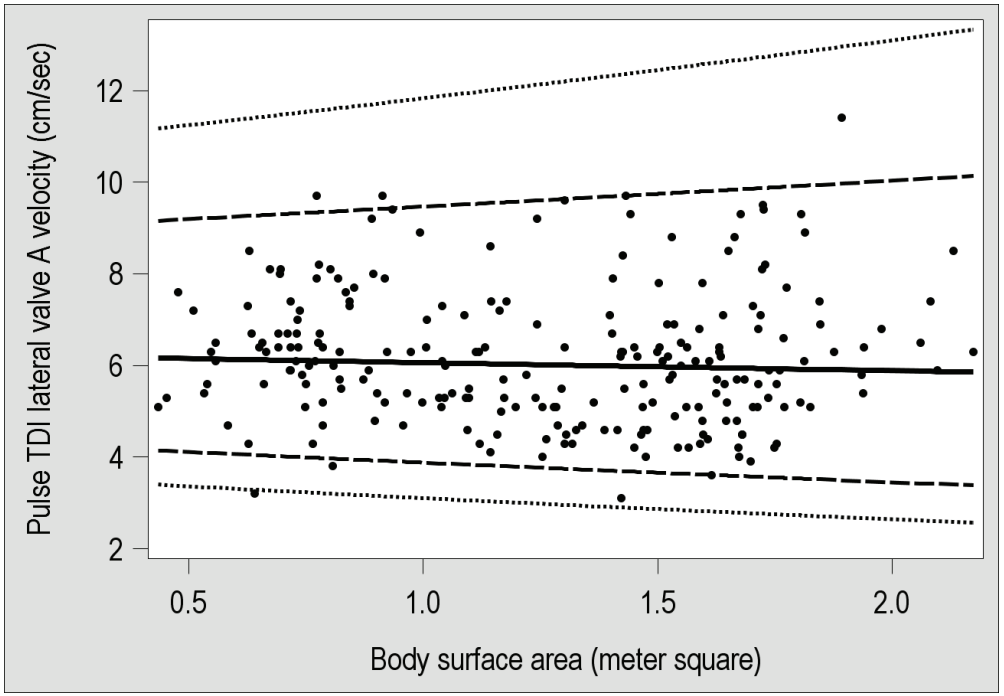

LV myocardial performance index
0.0
0.2
0.4
0.6
0.5
1.0
1.5
2.0
Body surface area (meter square)


Pulmonary vein A wave velocity (cm/sec)
10
20
30
40
0.5
1.0
1.5
2.0
Body surface area (meter square)

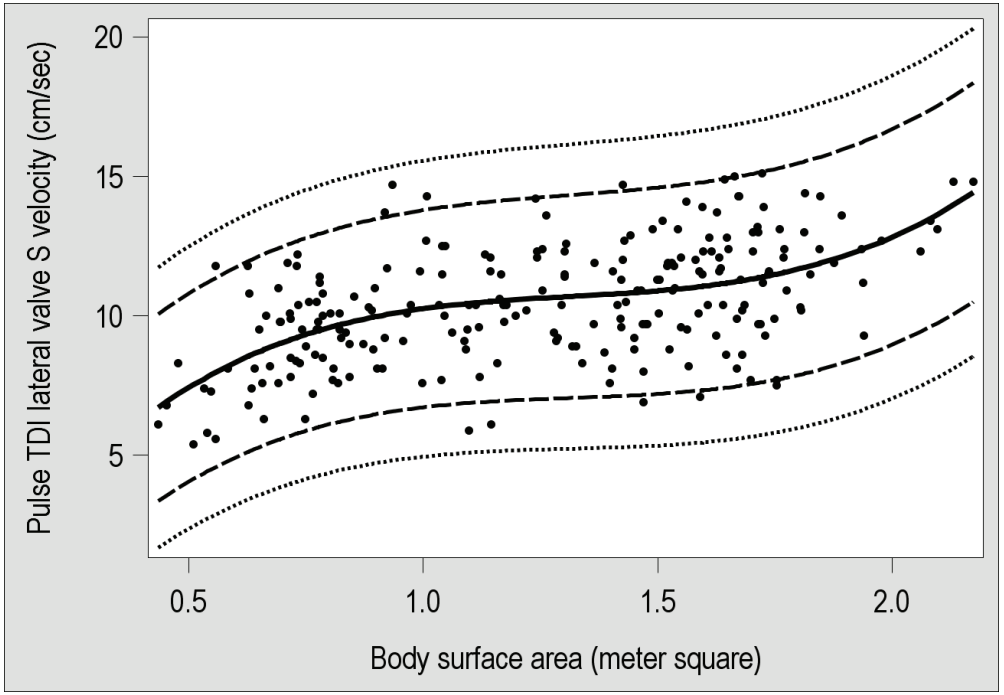

Pulmonary vein diastolic velocity (cm/sec)
40
60
80
100
0.5
1.0
1.5
2.0
Body surface area (meter square)


Pulmonary vein systolic velocity (cm/sec)
20
40
60
80
100
0.5
1.0
1.5
2.0
Body surface area (meter square)

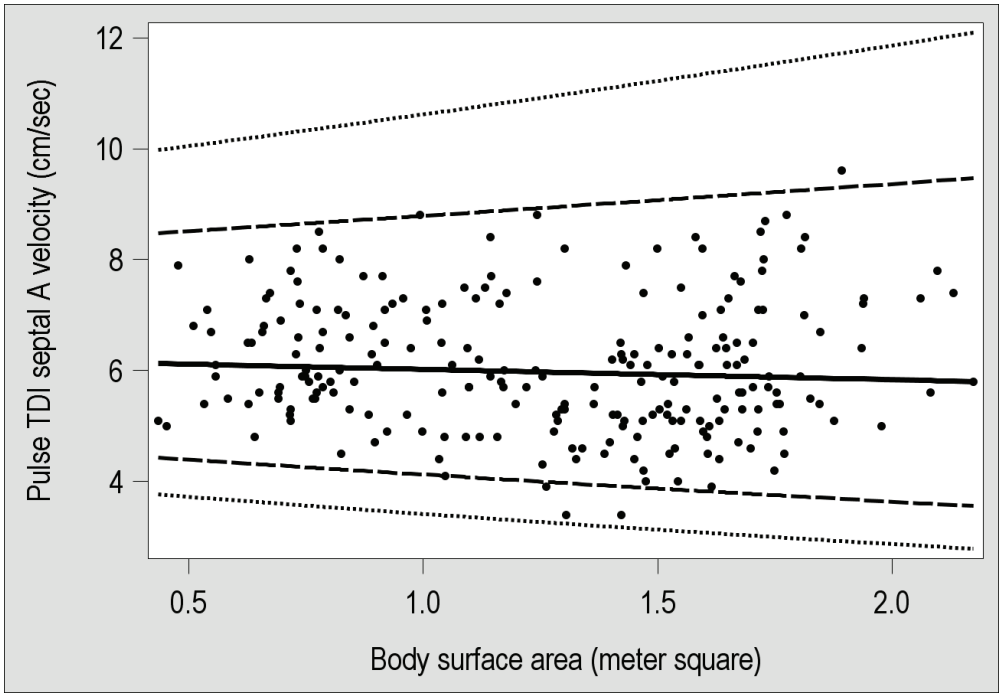

Pulmonary vein A wave duration (msec)
200
150
100
50
0
0.5
1.0
1.5
2.0
Body surface area (meter square)

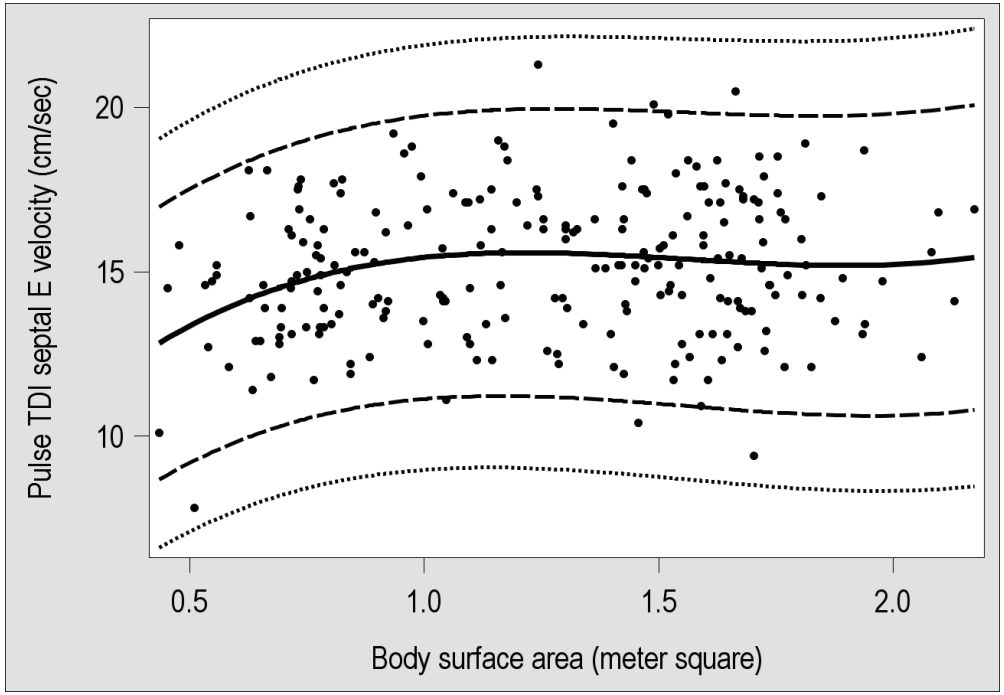

Pulse TDI lateral valve A velocity (cm/sec)
12
10
8
6
4
2
0.5
1.0
1.5
2.0
Body surface area (meter square)

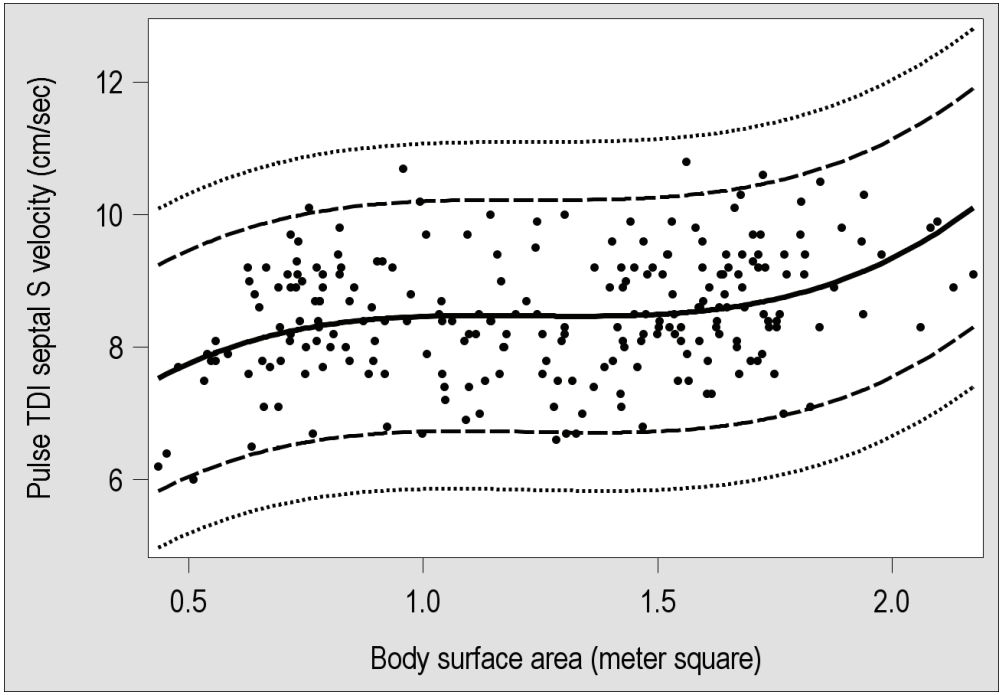

Pulse TDI lateral E velocity (cm/sec)
25
20
15
10
5
0.5
1.0
1.5
2.0
Body surface area (meter square)

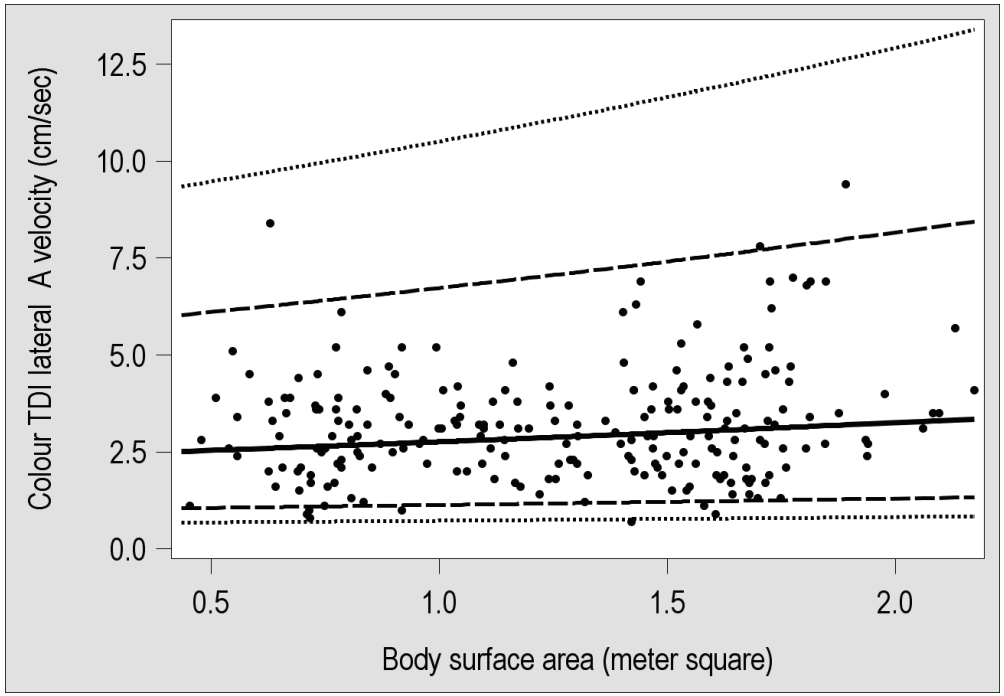

Pulse TDI lateral valve S velocity (cm/sec)
20
15
10
5
0.5
1.0
1.5
2.0
Body surface area (meter square)

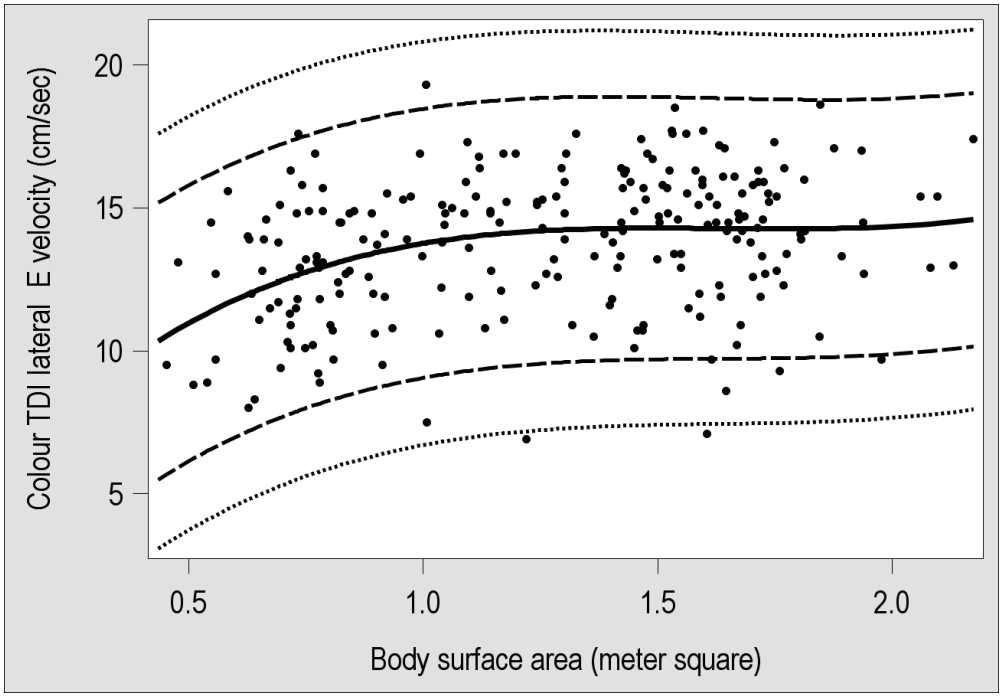

Lateral E/E' ratio
10
8
6
4
2
0.5
1.0
1.5
2.0
Body surface area (meter square)

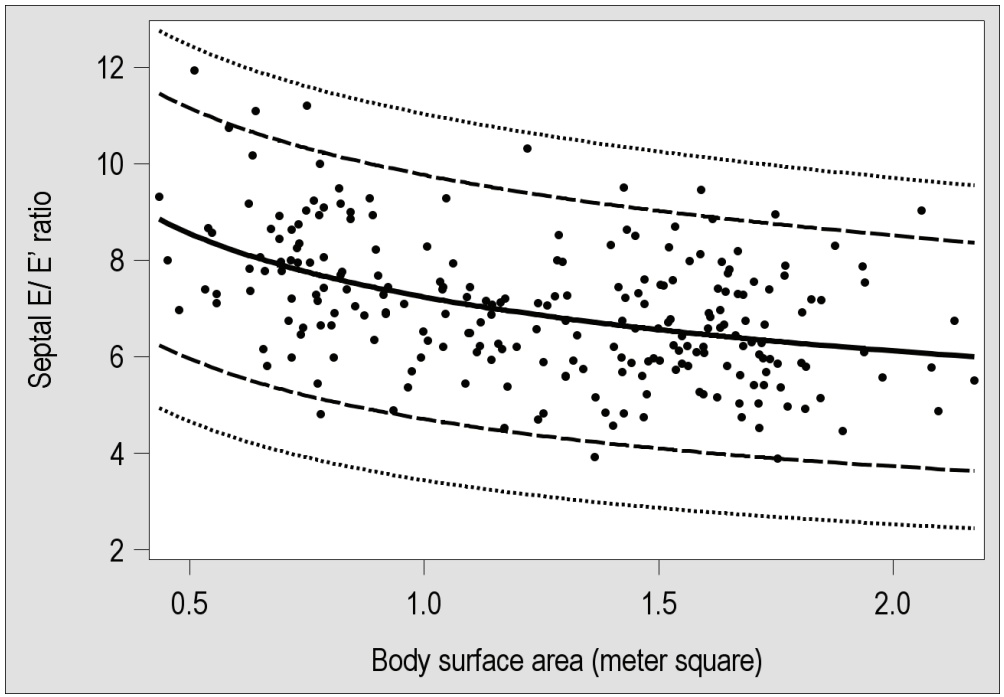

Pulse TDI septal A velocity (cm/sec)
12
10
8
6
4
0.5
1.0
1.5
2.0
Body surface area (meter square)

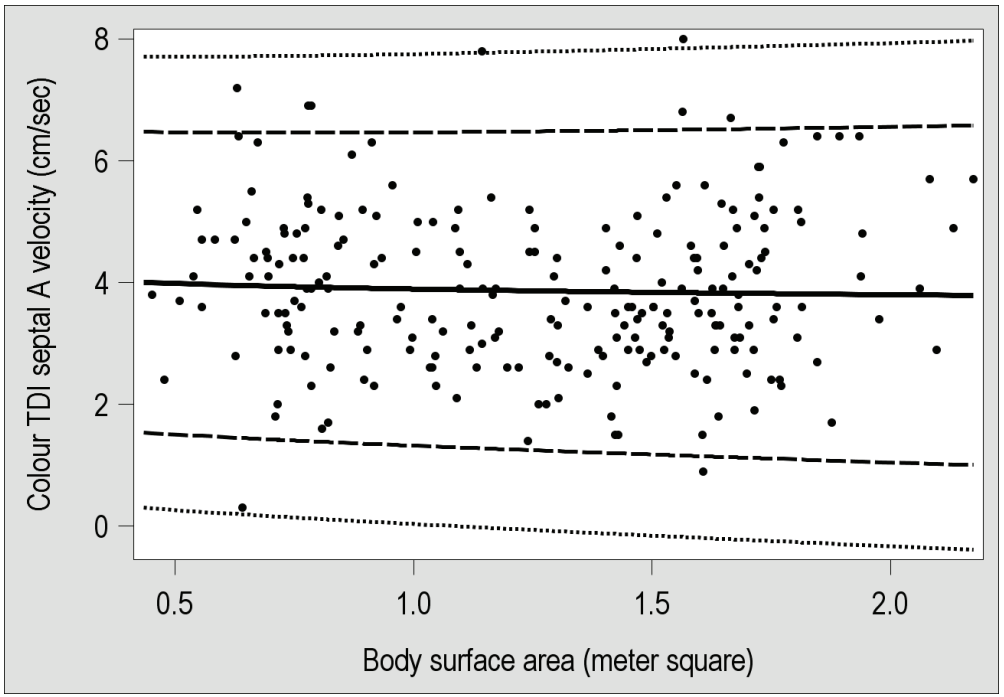

Pulse TDI septal E velocity (cm/sec)
20
15
10
0.5
1.0
1.5
2.0
Body surface area (meter square)

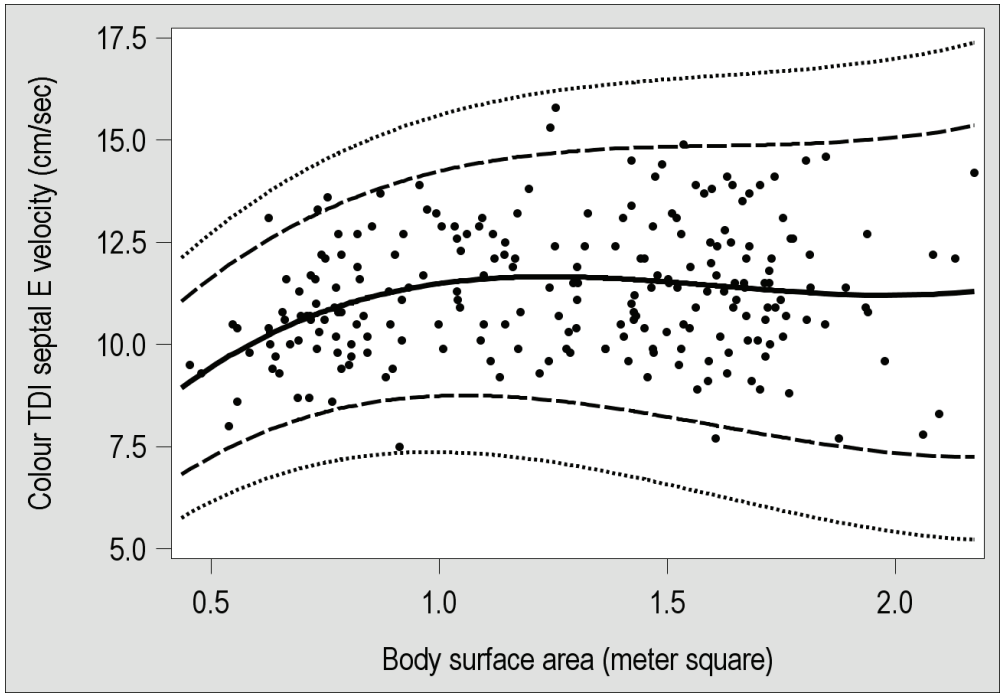

Pulse TDI septal S velocity (cm/sec)
12
10
8
6
0.5
1.0
1.5
2.0
Body surface area (meter square)

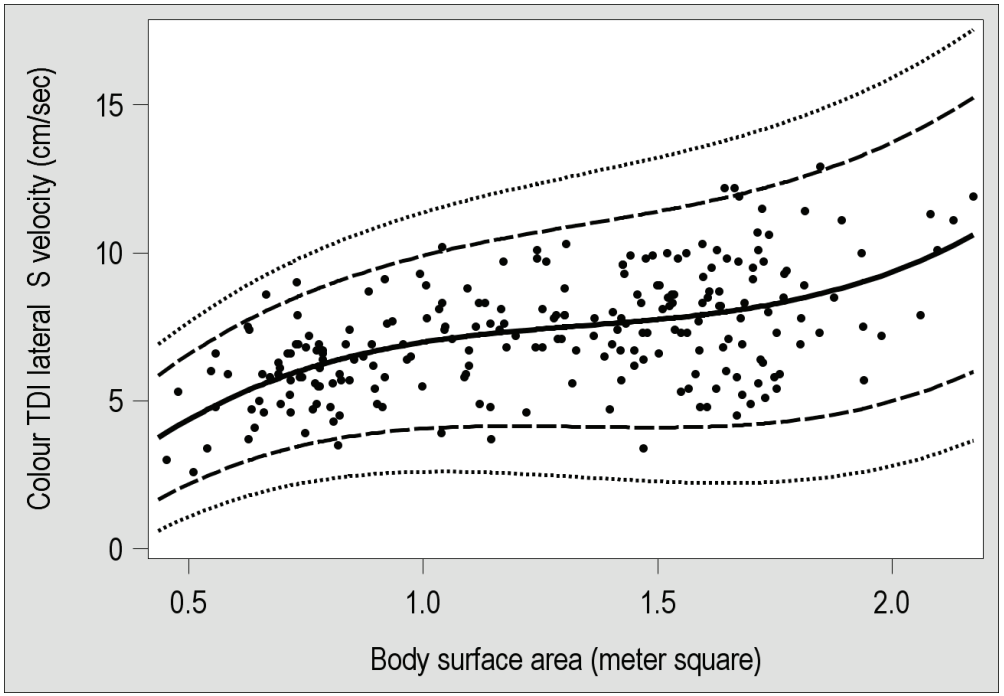

Colour TDI lateral A velocity (cm/sec)
12.5
10.0
7.5
5.0
2.5
0.0
0.5
1.0
1.5
2.0
Body surface area (meter square)

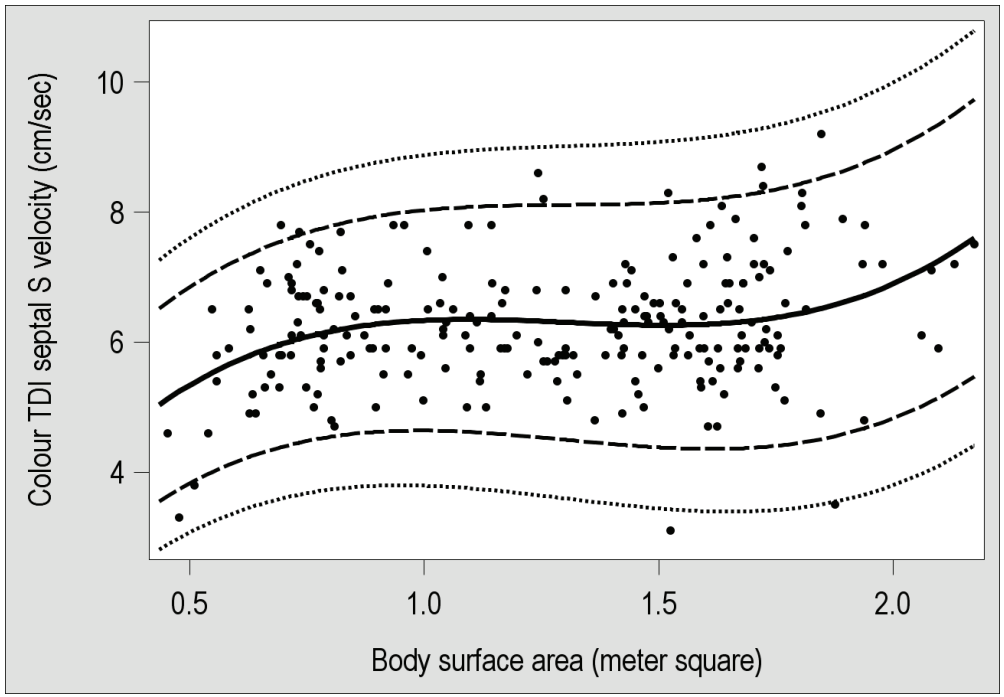

Colour TDI lateral E velocity (cm/sec)
20
15
10
5
0.5
1.0
1.5
2.0
Body surface area (meter square)


Septal E/ E' ratio
12
10
8
6
4
2
0.5
1.0
1.5
2.0
Body surface area (meter square)


Colour TDI septal A velocity (cm/sec)
8
6
4
2
0
0.5
1.0
1.5
2.0
Body surface area (meter square)


Colour TDI septal E velocity (cm/sec)
17.5
15.0
12.5
10.0
7.5
5.0
0.5
1.0
1.5
2.0
Body surface area (meter square)


Colour TDI lateral S velocity (cm/sec)
15
10
5
0
0.5
1.0
1.5
2.0
Body surface area (meter square)


Colour TDI septal S velocity (cm/sec)
10
8
6
4
0.5
1.0
1.5
2.0
Body surface area (meter square)